Realistic model of the nucleon spectral function in few- and many-nucleon systems

C. Ciofi degli Atti
Department of Physics, University of Perugia and Istituto Nazionale di Fisica Nucleare, Sezione di Perugia, Via A. Pascoli, I-06100 Perugia, Italy

S. Simula
Istituto Nazionale di Fisica Nucleare, Sezione Sanitá, Viale Regina Elena 299, I-00161 Roma, Italy
(Received 13 July 1995)

By analyzing the high-momentum features of the nucleon momentum distribution in light and complex nuclei, it is argued that the basic two-nucleon configurations generating the structure of the nucleon spectral function at high values of the nucleon momentum and removal energy can be properly described by a factorized ansatz for the nuclear wave function, which leads to a nucleon spectral function in the form of a convolution integral involving the momentum distributions describing the relative and center-of-mass motion of a correlated nucleon-nucleon pair embedded in the medium. The spectral functions of ^{3}He and infinite nuclear matter resulting from the convolution formula and from many-body calculations are compared, and a very good agreement in a wide range of values of nucleon momentum and removal energy is found. Applications of the model to the analysis of inclusive and exclusive processes are presented, illustrating those features of the cross section which are sensitive to that part of the spectral function which is governed by short-range and tensor nucleon-nucleon correlations.

PACS number(s): 21.10.Jx, 21.65.+f, 24.10.Cn, 27.10.+h

I. INTRODUCTION

The nucleon spectral function $P(k,E)$ represents the joint probability to find in a nucleus a nucleon with momentum $k \equiv |\vec{k}|$ and removal energy E, and therefore it provides fundamental information on the dynamics of the nucleon in the nuclear medium. Since the momentum and removal energy dependencies of $P(k,E)$ are governed by the single particle features of nuclear structure as well as by the behavior of the nuclear wave function at short nucleon-nucleon (NN) separations (see Ref. [1]), the relevance of the experimental and theoretical investigations of $P(k,E)$ is clear.

As far as the experimental investigation is concerned, it is well known that within the impulse approximation the cross section for nucleon knockout processes is directly proportional to the nucleon spectral function, and, although final state interactions and meson exchange currents can destroy such a proportionality, several experiments have already provided relevant information on the general features of $P(k,E)$, e.g.: (i) the y-scaling analysis [2] of inclusive (e,e') experiments [3] has clarified the link between $P(k,E)$ and the nucleon momentum distribution $n(k)$; (ii) the high-resolution $A(e,e'p)X$ experiments have shown that the shell-model occupation numbers can be substantially less than one, which is a clear signature of the breakdown of the mean field picture [4]; (iii) the exclusive $A(e,e'p)X$ experiments on $A=3$ and $A=4$ nuclei, performed in kinematical regions corresponding to high excitation energies of the residual nuclear system, have given the first direct signature of the effects of NN correlations on $P(k,E)$ [5,6]; (iv) the recent data on the process $^{12}\mathrm{C}(e,e'p)X$ have raised the question of multinucleon emissions generated by NN correlations [7,8]. The above experimental information clearly indicates that the single-particle strength is not concentrated uniquely at low values of k and E (as it is the case within a mean field picture), but, due to short-range and tensor NN correlations, is spread over a wide range of nucleon momenta and removal energies.

As far as the theoretical investigation of the nucleon spectral function is concerned, the calculation of $P(k,E)$ for $A>2$ requires the knowledge of a complete set of wave functions for $(A-1)$ interacting nucleons. Thus, since the latter ones should be obtained from many-body calculations using realistic models of the NN interaction, the evaluation of $P(k,E)$ represents a formidable task. In case of ^{3}He the nucleon spectral function has been obtained using three-body Faddeev [9] or variational [10] wave functions, whereas for $A=\infty$ the evaluation of $P(k,E)$ has been performed using the orthogonal correlated basis approach [11] and perturbation expansions of the one-nucleon propagator [12–16]. It should be mentioned that $P(k,E)$ has also been obtained for $A=4$ [17] using a plane-wave approximation for the final states of the three-nucleon continuum. Finally, it is only recently that the results of the investigation within a G-matrix perturbation theory of the effects of the short-range and tensor NN correlations on the p-wave single-particle spectral function of ^{16}O, have been reported [18]. Thus microscopic calculations of the full nucleon spectral function of light and complex nuclei are still called for, and it is for this reason that the development of models of $P(k,E)$ is useful and necessary.

In Ref. [1] a model of the nucleon spectral function has been proposed according to which, at high values of the nucleon momentum and removal energy, $P(k,E)$ is expressed as a convolution integral of the momentum distributions describing the relative and center-of-mass (CM) motion of a correlated NN pair. The basic assumption of the model is that the high momentum and high removal energy parts of the nucleon spectral function are generated by ground-state

configurations in which two nucleons are very close and form a correlated pair, whose CM is, at the same time, far apart from the other $(A-2)$ nucleons. This means that the two nucleons in the pair have large relative momenta (i.e., $k_{\rm rel}\equiv|\vec{k}_1-\vec{k}_2|/2>0.3$ GeV/$c\sim k_F$), whereas the CM momentum of the pair is a low one ($k_{\rm CM}\equiv|\vec{k}_1+\vec{k}_2|<0.3$ GeV/c). It has been shown [1] that such a model satisfactorily reproduces the spectral function of ^{3}He and nuclear matter calculated within many-body approaches using realistic models of the NN interaction. However, a comprehensive derivation of the model for complex nuclei was not presented in Ref. [1]; thus the aim of this paper is to provide the general formulation of the convolution model and to apply it both to few-nucleon systems and complex nuclei.

The paper is organized as follows. In Sec. II the definition of $P(k,E)$ as well as its general form for uncorrelated and correlated many-nucleon systems are recalled; since our model for the spectral function relies on some peculiar features of the nucleon momentum distributions and their relationships with the spectral function, in Sec. II this matter will be also discussed in some details. In Sec. III the convolution model of $P(k,E)$ sketched in Ref. [1] is extended to any value of the mass number A. In Sec. IV the predictions of our model both for few-nucleon systems and complex nuclei are presented and compared with available many-body calculations. In Secs. V and VI some applications of our model to the analysis of inclusive and exclusive quasielastic electron scattering are presented. Finally, the summary and the conclusions are presented in Section VII.

II. GENERAL THEORETICAL FRAMEWORK: THE SPECTRAL FUNCTION AND THE NUCLEON MOMENTUM DISTRIBUTION

A. General definitions

The nucleon spectral function $P(k,E)$ gives the joint probability to find in a nucleus a nucleon with momentum k and removal energy E. Since the latter is defined as $E\equiv|E_A|-|E_{A-1}|+E^*_{A-1}$[E^*_{A-1} being the (positive) excitation energy of the system with $(A-1)$ nucleons measured with respect to its ground state, and E_A (E_{A-1}) the binding energy of the nucleus A $(A-1)$], the spectral function also represents the probability that, after a nucleon with momentum k is removed from the target, the residual $(A-1)$-nucleon system is left with excitation energy E^*_{A-1}. Adopting a nonrelativistic Schrödinger description of nuclei, the nucleon spectral function is defined as follows:

$$P(k,E)=\frac{1}{2J_0+1}\sum_{M_0\sigma}\langle\Psi^0_A|a^\dagger_{\vec{k},\sigma}\delta[E-(H-E_A)]a_{\vec{k},\sigma}|\Psi^0_A\rangle, \tag{1}$$

where $a^\dagger_{\vec{k},\sigma}$ ($a_{\vec{k},\sigma}$) is the creation (annihilation) operator of a nucleon with momentum $\vec{k}$ and spin projection σ; Ψ^0_A is the intrinsic eigenfunction of the ground state of the nuclear Hamiltonian H with eigenvalue E_A and total angular momentum (and its projection) J_0 (M_0). Note that, being Ψ^0_A an intrinsic wave function, the motion of the center of mass of the residual system cannot contribute to Eq. (1). Note, moreover, that both $\vec{k}$ and E are intrinsic quantities; the former one is the internal momentum conjugate to the relative distance $\vec{z}$ between the nucleon and the center of mass of the $(A-1)$ system, and the latter is directly related to the intrinsic quantity E^*_{A-1} by $E=E_{A-1}-E_A+E^*_{A-1}\equiv E_{\rm min}+E^*_{A-1}$, where $E_{\rm min}\equiv|E_A|-|E_{A-1}|$ is the (positive) minimum value of the removal energy. Using the completeness relation $\Sigma_f|\Psi^f_{A-1}\rangle\langle\Psi^f_{A-1}|=1$ for the final states of the residual system, one has

$$P(k,E)\equiv\frac{1}{2J_0+1}\sum_{M_0\sigma}\sum_f|\langle\Psi^f_{A-1}|a_{\vec{k},\sigma}|\,\Psi^0_A\rangle|^2\times\delta[E-(E^f_{A-1}-E_A)], \tag{2}$$

where Ψ^f_{A-1} is the intrinsic eigenfunction of the state f of the Hamiltonian H_{A-1} with eigenvalue $E^f_{A-1}\equiv E_{A-1}+E^*_{A-1}$. Introducing the overlap integral $G^\sigma_{f0}(\vec{z})$ defined as

$$G^\sigma_{f0}(\vec{z})\equiv\int d\vec{x}\ldots d\vec{y}[\chi^{1/2}_\sigma\Psi^f_{A-1}(\vec{x}\ldots\vec{y})]^*\Psi^0_A(\vec{x}\ldots\vec{y},\vec{z}), \tag{3}$$

where $\chi^{1/2}_\sigma$ is the two-component Pauli spinor of the nucleon, one has (cf. Ref. [10])

$$P(k,E)=\frac{1}{(2\pi)^3}\frac{1}{2J_0+1}\sum_{M_0\sigma}\sum_f\left|\int d\vec{z}\ e^{i\vec{k}\cdot\vec{z}}G^\sigma_{f0}(\vec{z})\right|^2\times\delta[E-(E^f_{A-1}-E_A)]. \tag{4}$$

B. The nucleon spectral function for uncorrelated and correlated many-nucleon systems

From Eq. (4) it follows that the nucleon spectral function can be represented in the following form (cf. [19])

$$P(k,E)=P_0(k,E)+P_1(k,E), \tag{5}$$

with

$$P_0(k,E)\equiv\frac{1}{(2\pi)^3}\frac{1}{2J_0+1}\sum_{M_0\sigma}\sum_{f<c}\left|\int d\vec{z}\ e^{i\vec{k}\cdot\vec{z}}G^\sigma_{f0}(\vec{z})\right|^2\times\delta[E-(E^f_{A-1}-E_A)], \tag{6}$$

$$P_1(k,E)\equiv\frac{1}{(2\pi)^3}\frac{1}{2J_0+1}\sum_{M_0\sigma}\sum_{f>c}\left|\int d\vec{z}\ e^{i\vec{k}\cdot\vec{z}}G^\sigma_{f0}(\vec{z})\right|^2\times\delta[E-(E^f_{A-1}-E_A)], \tag{7}$$

where $f<c$ ($f>c$) means that all final states of the residual system below (above) the continuum threshold are considered, i.e., in $P_0(k,E)$ only final states corresponding to the discrete spectrum of H_{A-1} are included, whereas all final states belonging to the continuum spectrum of H_{A-1} contribute to $P_1(k,E)$.

Let us now consider the predictions of the mean field approach for the nucleon spectral function. If we consider the nucleus as an ensemble of independent nucleons filling shell-

model states α with momentum distributions n_α and single-particle energies ε_α, one has[1]

$$P_0^{(\mathrm{SM})}(k,E)=\frac{1}{4\pi A}\sum_\alpha A_\alpha n_\alpha^{(\mathrm{SM})}(k)\,\delta[E-|\varepsilon_\alpha|] \qquad (8)$$

and

$$P_1^{(\mathrm{SM})}(k,E)=0. \qquad (9)$$

In Eq. (8) A_α is the number of nucleons in the state α ($\Sigma_\alpha A_\alpha=A$) and the sum over α runs only over hole states of the target, which means that the occupation probability S_α is

$$S_\alpha^{(\mathrm{SM})}\equiv\int_0^\infty dk\ k^2 n_\alpha^{(\mathrm{SM})}(k)=1 \quad \text{for} \quad \alpha<\alpha_F$$
$$=0 \quad \text{for} \quad \alpha>\alpha_F. \qquad (10)$$

In the limit $A\to\infty$, the nucleon spectral function for a non-interacting Fermi gas is given by

$$P_0^{(\mathrm{FG})}(k,E)=\frac{3}{4\pi k_F^3}\,\theta(k_F-k)\,\delta\left[E+\frac{k^2}{2M}\right],$$

$$P_1^{(\mathrm{FG})}(k,E)=0, \qquad (11)$$

which implies that the occupation probability for the single-particle plane-wave states is equal to 1 for $k\leqslant k_F$ and 0 for $k>k_F$.

The main effect of NN correlations is to deplete states below the Fermi level and to make the states above the Fermi level partially occupied. By such a mechanism $P_0(k,E)\neq P_0^{\mathrm{SM}}(k,E)$ and $P_1(k,E)\neq 0$. Disregarding the finite width of the states below the Fermi level, the (modified) shell-model contribution can be written as

$$P_0(k,E)=\frac{1}{4\pi A}\sum_{\alpha<\alpha_F} A_\alpha n_\alpha(k)\,\delta[E-|\varepsilon_\alpha|], \qquad (12)$$

where the occupation probability for hole states ($\alpha<\alpha_F$) is

$$S_\alpha=\int_0^\infty dk\ k^2 n_\alpha(k)<1. \qquad (13)$$

In case of nuclear matter one has [11]

$$P_0(k,E)=\frac{3}{4\pi k_F^3}Z(k)\,\theta(k_F-k)\,\delta[E+e_v(k)], \qquad (14)$$

where $Z(k)$ is the hole strength and $e_v(k)$ is the hole single-particle energy spectrum [in absence of NN correlations $e_v(k)=k^2/2M$ and $Z(k)=1$, so that the Fermi gas spectral function (Eq. (11)) is recovered]. As for $P_1(k,E)$, its general expression reads as follows:

$$P_1(k,E)=\frac{1}{(2\pi)^3}\frac{1}{2J_0+1}\sum_{M_0\sigma}\sum_{f\neq\{\alpha<\alpha_F\}}\left|\int d\vec{z}\ e^{i\vec{k}\cdot\vec{z}}G_{f0}^{\sigma}(\vec{z})\right|^2$$
$$\times\,\delta[E-(E_{A-1}^f-E_{A-1})], \qquad (15)$$

where more complex configurations of the $(A-1)$-nucleon system are included, like, e.g., one-particle—two-hole states which can be reached when two-particle—two-hole states in the target nucleus are considered. In such a way, the main effects of NN correlations on $P_1(k,E)$ is to generate high momentum and high removal energy components.

Before closing this subsection, let us consider explicitly the case of nuclei with $A\leqslant 4$, for in this case the mean field picture underlying Eq. (12) is not a realistic one. In case of the deuteron there is only one possible final state, because the residual $(A-1)$ system is just a nucleon; this means that $P_1(k,E)$ for $A=2$ is identically vanishing, even in presence of NN correlations. Thus the dependence of $P(k,E)$ upon the removal energy is simply given by a delta function. Explicitly, the nucleon spectral function of the deuteron reads as follows:

$$P(k,E)=\frac{1}{4\pi}n^{(D)}(k)\,\delta[E-E_{\min}], \qquad (16)$$

where $E_{\min}=2.226$ MeV is the deuteron binding energy and $n^{(D)}(k)$ is the nucleon momentum distribution in the deuteron (see the next subsection). In case of helium nuclei the residual $(A-1)$-nucleon system has only one bound state, namely the ground state of the two- and three-nucleon system for $A=3$ and $A=4$, respectively. Thus Eq. (6) yields the nucleon spectral function associated to the ground-to-ground transition, viz.

$$P_0(k,E)=\frac{1}{(2\pi)^3}\frac{1}{2J_0+1}\sum_{M_0\sigma}\left|\int d\vec{z}\ e^{i\vec{k}\cdot\vec{z}}G_{00}^{\sigma}(\vec{z})\right|^2$$
$$\times\,\delta[E-E_{\min}], \qquad (17)$$

where $E_{\min}\equiv|E_A|-|E_{A-1}|$ equals to 5.5 MeV and 19.8 MeV in case of ^{3}He and ^{4}He, respectively. As far as $P_1(k,E)$ is concerned, it is given by

$$P_1(k,E)=\frac{1}{(2\pi)^3}\frac{1}{2J_0+1}\sum_{M_0\sigma}\sum_{f\neq 0}\left|\int d\vec{r}\ e^{i\vec{k}\cdot\vec{r}}G_{f0}^{\sigma}(\vec{r})\right|^2$$
$$\times\,\delta[E-(E_{A-1}^f-E_{A-1})]. \qquad (18)$$

C. The spectral function and the nucleon momentum distribution

The nucleon momentum distribution $n(k)$ is defined as follows:

$$n(k)\equiv\frac{1}{2\pi^2}\int d\vec{z}\ d\vec{z}'\ e^{i\vec{k}\cdot(\vec{z}-\vec{z}')}\rho(\vec{z},\vec{z}'), \qquad (19)$$

where (omitting spin indices)

$$\rho(\vec{z},\vec{z}')\equiv\int d\vec{x}\ldots d\vec{y}\,[\Psi_A^0(\vec{x}\ldots\vec{y},\vec{z})]^*\Psi_A^0(\vec{x}\ldots\vec{y},\vec{z}') \qquad (20)$$

[1]In this paper the normalization of the nucleon momentum distribution $n(k)$ is chosen to be $\int_0^\infty dk\ k^2 n(k)=1$.

is the off-diagonal one-body density matrix. The calculation of $n(k)$ is simpler than the calculation of $P(k,E)$, for only the ground-state wave function is required. The relation between $n(k)$ and $P(k,E)$ can be easily obtained by inserting in Eq. (20) the completeness relation $\Sigma_f |\Psi^f_{A-1}\rangle\langle\Psi^f_{A-1}| = 1$ for the final states of the residual system and by using Eq. (4); one obtains the following momentum sum rule:

$$n(k) = 4\pi \int_{E_{\min}}^{\infty} dE\ P(k,E). \tag{21}$$

Using the decomposition given by Eq. (5), one has (cf. [20], [19])

$$n(k) = n_0(k) + n_1(k), \tag{22}$$

with

$$n_0(k) \equiv 4\pi \int_{E_{\min}}^{\infty} dE\ P_0(k,E) = \frac{1}{2\pi^2} \frac{1}{2J_0+1} \sum_{M_0\sigma} \sum_{f=\{\alpha<\alpha_F\}} \left| \int d\vec{z}\ e^{i\vec{k}\cdot\vec{z}} G^{\sigma}_{f0}(\vec{z}) \right|^2, \tag{23}$$

$$n_1(k) \equiv 4\pi \int_{E_{\min}}^{\infty} dE\ P_1(k,E) = \frac{1}{2\pi^2} \frac{1}{2J_0+1} \sum_{M_0\sigma} \sum_{f\neq\{\alpha<\alpha_F\}} \left| \int d\vec{z}\ e^{i\vec{k}\cdot\vec{z}} G^{\sigma}_{f0}(\vec{z}) \right|^2. \tag{24}$$

For $A=3$ and $A=4$, one gets [cf. Eq. (17)]

$$n_0(k) = \frac{1}{2\pi^2} \frac{1}{2J_0+1} \sum_{M_0\sigma} \left| \int d\vec{z}\ e^{i\vec{k}\cdot\vec{z}} G^{\sigma}_{00}(\vec{z}) \right|^2, \tag{25}$$

whereas for a complex nucleus, when NN correlations are considered, one has [cf. Eq. (12)]

$$n_0(k) = \frac{1}{4\pi A} \sum_{\alpha<\alpha_F} A_\alpha n_\alpha(k). \tag{26}$$

It can be seen therefore that in both cases there is a direct relationship between $P_0(k,E)$ and $n_0(k)$, viz.

$$P_0(k,E) = \frac{1}{4\pi} n_0(k)\, \delta[E - E_{\min}] \tag{27}$$

for a few-body system, and Eq. (12) for a complex nucleus. On the contrary, $P_1(k,E)$ cannot be expressed in terms of $n_1(k)$ both in case of light and complex nuclei.

The integration of $n_0(k)$ and $n_1(k)$ over the nucleon momentum yields the spectroscopic factors S_0 and S_1, respectively, viz.

$$S_0 \equiv \int_0^{\infty} dk\ k^2 n_0(k) = \sum_{\alpha<\alpha_F} S_\alpha, \qquad S_1 \equiv \int_0^{\infty} dk\ k^2 n_1(k), \tag{28}$$

with $S_0 + S_1 = 1$. Within the mean field picture one has $S_0 = 1$ and $S_1 = 0$. When NN correlations are considered, it turns out that the spectroscopic factor of the ground-to-ground transition S_0 is equal to $\simeq 0.65$ and $\simeq 0.8$ (implying $S_1 \simeq 0.35$ and $\simeq 0.2$) for ^{3}He [20] and ^{4}He [21,17], respectively, whereas the average depletion of single-particle states below Fermi level in complex nuclei is expected to be $S_0 \simeq 0.8$ in overall agreement with the results obtained from high-resolution exclusive experiments [4]. In case of the infinite nuclear matter the calculation of Ref. [22] yields $S_0 \simeq 0.75$, which means $S_1 \simeq 0.25$.

The nucleon momentum distribution $n(k)$ has been calculated for several nuclei, ranging from the deuteron to nuclear matter [20–29], using nonrelativistic ground-state wave functions with realistic models of the NN interaction (like, e.g., the Reid soft core interaction [30], the Paris potential [31], and the Argonne v_{14} interaction [32]) and considering also three-nucleon forces (cf. Ref. [23]). A sample of the results of those calculations is reported in Fig. 1, where it can be clearly seen that (i) the low-momentum part of $n(k)$ ($k < 1.5$ fm^{-1}) is almost totally exhausted by $n_0(k)$, which means that $n(k)$ at low momenta is dominated by the single-particle features of the nuclear structure; (ii) the high-momentum tail of $n(k)$ ($k > 1.5$ fm^{-1}) is entirely governed by $n_1(k)$, which at high momenta overwhelms the contribution from $n_0(k)$ by several orders of magnitude; this means that $n(k)$ at high momenta is governed by the short-range properties of nuclear structure; (iii) both at low and high momenta the results of the existing calculations of $n(k)$ agree fairly well with the general trend of the nucleon momentum distribution extracted from inclusive and exclusive experiments.

In Fig. 2(a) the nucleon momentum distributions calculated for complex nuclei are directly compared with the one of the deuteron. It can be clearly seen that the high-momentum tail of $n(k)$ at $k > 2$ fm^{-1} is similar for all nuclei and it is essentially given by the nucleon momentum distribution of the deuteron times an A-dependent scale factor. Therefore, the ratio of $n^A(k)$ for a nucleus A to $n^D(k)$ for the deuteron is expected to exhibit a plateau for $k > 2$ fm^{-1}, as it indeed appears in Fig. 2(b). The height of the plateau turns out to be ~ 2 for the proton in ^{3}He, ~ 4 in ^{4}He and ^{16}O, ~ 4.5 in ^{56}Fe, and ~ 5 in nuclear matter. The similarity between the high momentum parts of the momentum distributions for complex nuclei and the deuteron has been firstly illustrated in Ref. [28].

From the above considerations it follows that a simple model for the nucleon momentum distribution $n(k)$ could read as follows:

$$n(k) \simeq n_0(k) = \frac{1}{4\pi A} \sum_{\alpha<\alpha_F} A_\alpha n_\alpha(k) \quad \text{for } k < \tilde{k}, \qquad n(k) \simeq n_1(k) = C^A n_{\text{deut}}(k) \quad \text{for } k > \tilde{k}, \tag{29}$$

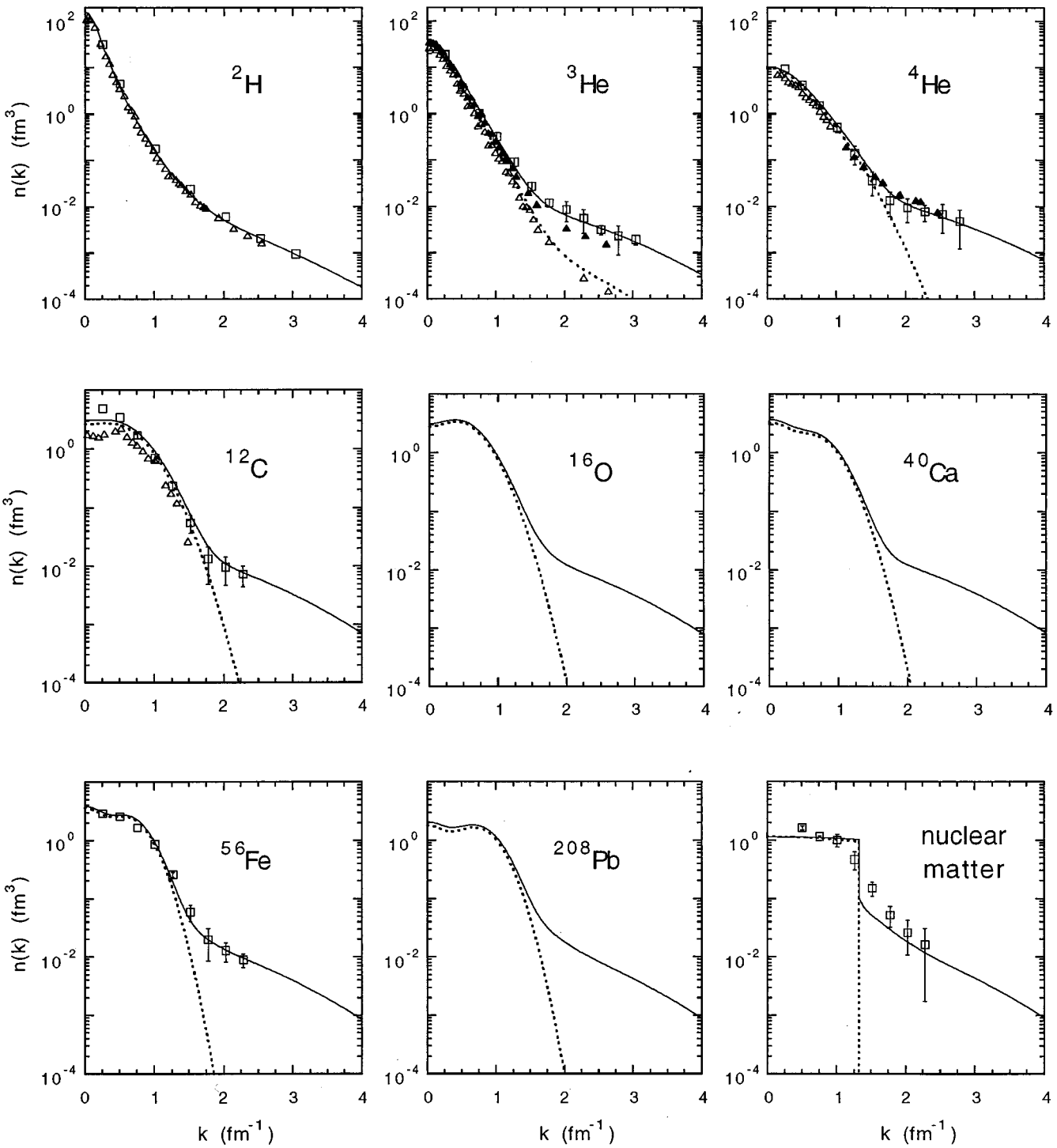

FIG. 1. The many-body nucleon momentum distribution $n(k)$ [Eq. (19)] corresponding to the parametrization described in the Appendix (solid lines). Considering the representation (22), the momentum distribution $n_0(k)$ [Eq. (25) for $A=3,4$ and Eq. (26) for complex nuclei] is given by the dotted lines. The deuteron momentum distribution has been calculated using the Paris potential [31] and the many-body results for the momentum distributions $n_0(k)$ and $n(k)$ have been taken from Refs. [20] (^{3}He) [23], (^{4}He) [24], (^{12}C and ^{40}Ca) [25], (^{16}O) [26], (^{56}Fe) [27], (^{208}Pb), and [22] (infinite nuclear matter). The normalization of $n(k)$ is $\int_0^\infty dk\, k^2 n(k)=1$. The theoretical calculations are compared with the experimental values of $n_0(k)$ and $n(k)$ extracted from the experimental data on inclusive $A(e,e')X$ and exclusive $A(e,e'p)X$ reactions. The open squares represent the results obtained within the y-scaling analysis of inclusive data for ^{2}H, ^{3}He, ^{4}He, ^{12}C, ^{56}Fe and nuclear matter performed in Ref. [2], and the full triangles are the results for $n(k)$ in ^{4}He extracted from the exclusive reaction ^{4}He$(e,e'p)X$ [6]. The open triangles represent the values of $n_0(k)$ obtained from the exclusive experiments off ^{2}H [33], ^{3}He [5], ^{4}He [34], and ^{12}C [35].

where $\tilde{k}\simeq 2.0$ fm^{-1}. We have parametrized the results of many-body calculations for $n_0(k)$ and $n_1(k)$, shown in Fig.1, using simple functional forms inspired by Eq. (29) (cf. Appendix).

In what follows we will make use of two important quantities, viz. the relative and center-of-mass (CM) momentum distributions of a two-nucleon cluster (N_1N_2), which are defined as follows:

$$n_{\rm rel}^{N_1N_2}(\vec{k}_{\rm rel})=\int d\vec{k}_{\rm CM}\; n^{N_1N_2}\left(\vec{k}_{\rm rel}+\frac{\vec{k}_{\rm CM}}{2},-\vec{k}_{\rm rel}+\frac{\vec{k}_{\rm CM}}{2}\right), \tag{30}$$

$$n_{\rm CM}^{N_1N_2}(\vec{k}_{\rm CM})=\int d\vec{k}_{\rm rel}\; n^{N_1N_2}\left(\vec{k}_{\rm rel}+\frac{\vec{k}_{\rm CM}}{2},-\vec{k}_{\rm rel}+\frac{\vec{k}_{\rm CM}}{2}\right), \tag{31}$$

where $\vec{k}_{\rm rel}\equiv(\vec{k}_1-\vec{k}_2)/2$ and $\vec{k}_{\rm CM}\equiv\vec{k}_1+\vec{k}_2$ are the relative and CM momentum of the pair N_1N_2, respectively, with $\vec{k}_1$ and $\vec{k}_2$ being measured from the CM of the system. In Eq. (30) $n^{N_1N_2}(\vec{k}_1,\vec{k}_2)$ is the two-nucleon momentum distribution

$$n^{N_1N_2}(\vec{k}_1,\vec{k}_2)\equiv\frac{1}{(2\pi)^6}\int d\vec{z}_1\; d\vec{z}_2\; d\vec{z}_1'\; d\vec{z}_2'\; e^{i\vec{k}_1\cdot(\vec{z}_1-\vec{z}_1')}\times e^{i\vec{k}_2\cdot(\vec{z}_2-\vec{z}_2')}\rho^{N_1N_2}(\vec{z}_1,\vec{z}_2;\vec{z}_1',\vec{z}_2'), \tag{32}$$

where

$$\rho^{N_1N_2}(\vec{z}_1,\vec{z}_2;\vec{z}_1',\vec{z}_2')\equiv\int d\vec{x}\ldots d\vec{y}[\Psi_A^0(\vec{x}\ldots\vec{y},\vec{z}_1,\vec{z}_2)]^*\times\Psi_A^0(\vec{x}\ldots\vec{y},\vec{z}_1',\vec{z}_2') \tag{33}$$

is the off-diagonal two-body density matrix. It should be pointed out that the evaluation of both $n_{\rm rel}^{N_1N_2}$ and $n_{\rm CM}^{N_1N_2}$ requires the knowledge of the ground-state wave function only. Till now, calculations of the relative and CM momentum distributions, obtained within many-body approaches, have been reported only for $A=3$ [9] and $A=4$ [36].

Before closing this subsection, we would like to mention that all the calculations of $n(k)$ considered in this paper are based on the use of a non-relativistic nuclear wave function. It is only recently that estimates of the relativistic corrections to the nuclear Hamiltonian has been calculated in case of light nuclei [37]; however, the effects of such corrections on $n(k)$ turns out to be quite small up to $k\sim4-5$ fm^{-1}, which is just the limit considered in this paper.

D. The saturation of the momentum sum rule

In Ref. [20] a relevant relationship between high momentum and high removal energy components has been for the first time illustrated by considering the partial momentum distribution $n_f(k)$, defined as follows:

$$n_f(k)\equiv4\pi\int_{E_{\rm min}}^{E_f}dE\; P(k,E), \tag{34}$$

where the upper limit of integration E_f can be varied from $E_{\rm min}$ to ∞. By definition, the partial momentum distribution $n_f(k)$ represents that part of $n(k)$ which is due to final $(A-1)$-nucleon states with $E\leq E_f$. When $E_f\to\infty$, one gets $n_f(k)\to n(k)$, and the momentum sum rule [Eq. (21)] is recovered. Thus the behavior of $n_f(k)$ as a function of E_f provides information on the saturation of the momentum sum rule and the relevance of binding effects. The calculation of $n_f(k)$ clearly requires the knowledge of the nucleon spectral function and, therefore, till now has been performed only for $A=3$ and $A=\infty$. The results of [20] for ^{3}He are reported in Fig. 3(a) for various values of E_f. It can be seen that at low values of k (<1.5 fm^{-1}) the momentum sum rule is saturated already at values of E_f very close to $E_{\rm min}$; this is not surprising, for at low momenta the nucleon spectral function is dominated by its component $P_0(k,E)$, whose strength is almost totally concentrated at low values of the removal energy [cf. Eq. (17) for ^{3}He and also Eq. (14) in case of infinite nuclear matter]. On the contrary, at high values of k (>1.5 fm^{-1}) the momentum sum rule is saturated only when high values of E_f are considered in Eq. (34); one finds that the higher the value of k the higher the value of E_f needed to saturate the momentum sum rule. These features of the saturation of the momentum sum rule at high momenta are due to the fact that the correlated part $P_1(k,E)$ of the spectral function is spread over a wide range of values of E for a given k, in agreement with the theoretical predictions of many-body approaches (see Ref. [1]) as well as with the experimental data on the exclusive processes ^{3}He$(e,e'p)X$ [5] and ^{4}He$(e,e'p)X$ [6], in which the removal energy and momentum dependencies of the nucleon emission roughly follow the kinematics of the emission from a two-nucleon system. Recently, such an important feature of the saturation of the momentum sum rule at high momenta has been also demonstrated for infinite nuclear matter in Ref. [11], as exhibited in Fig. 3(b).

III. THE CONVOLUTION MODEL FOR THE NUCLEON SPECTRAL FUNCTION

To develop our model spectral function, we make use of the two main results emerging from the analysis of existing calculations of $n(k)$ and $n_f(k)$ presented in the previous section, namely (i) the ''deuteronlike'' tail of $n(k)$, i.e., the observation that, apart from an overall scale factor, the behavior of $n(k)$ at high momenta ($k>2$ fm^{-1}) is almost independent of the atomic weight A; (ii) the saturation of the momentum sum rule at high momenta, which clearly indicates the strong link between high momentum and high removal energy components of the nuclear wave function, which are both generated by NN correlations. Both features should reflect some local properties of the NN wave function in the nuclear medium at short internucleon separations.

A. The two-nucleon correlation model

The analysis of the momentum distributions and the saturation of the momentum sum rule presented in Sec. II, show that high momentum and high removal energy components in nuclei are generated by NN correlations resembling the ones acting in a deuteron, with the many body aspects appearing through the constant C^A [cf. Eq. (29)] and the rich spectrum of removal energy values of the spectral function for an $A>2$ nucleus. A first microscopic model of NN correlations generating both high momentum and high removal energy components has been proposed in [38], where, by analyzing the perturbative expansion of the NN interaction and the nucleon momentum distribution for NN potentials

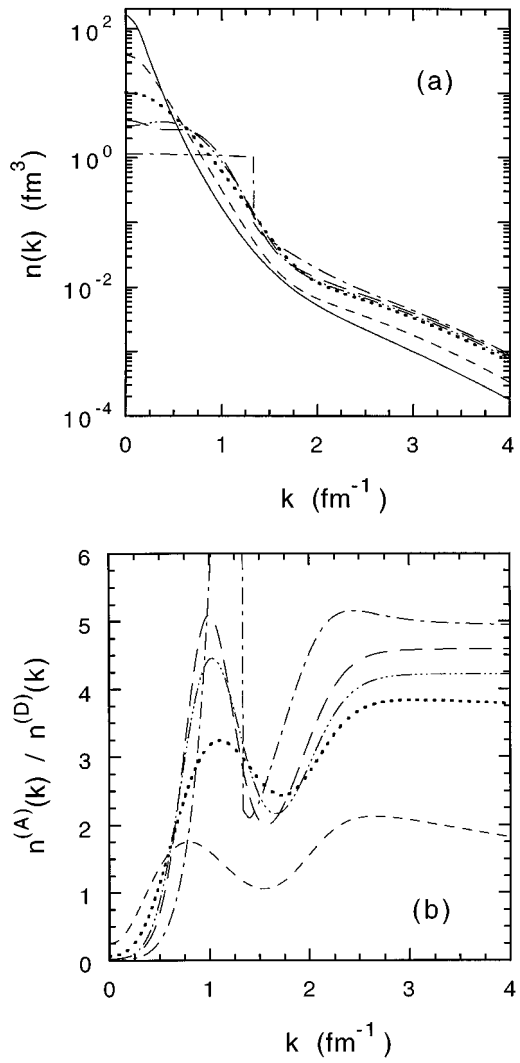

FIG. 2. The nucleon momentum distributions of Fig. 1 shown all together (a) and their ratio to the deuteron momentum distribution $n^{(D)}(k)$ (b). The solid, dashed, dotted, dot-dashed, long dashed, dot-long dashed lines correspond to ^{2}H, ^{3}He, ^{4}He, ^{16}O, ^{56}Fe, and nuclear matter, respectively.

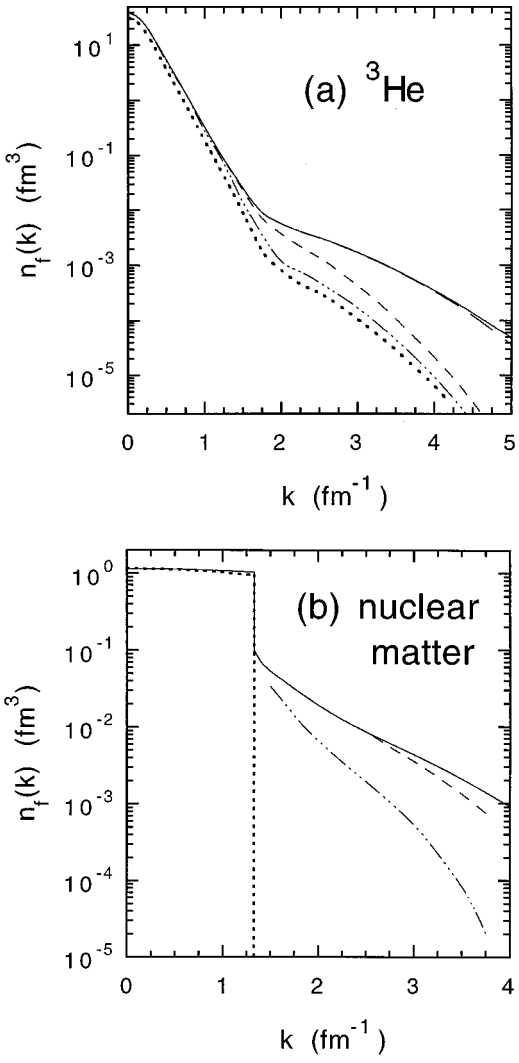

FIG. 3. The saturation of the momentum sum rule in ^{3}He (a) and infinite nuclear matter (b). The dotted and solid lines correspond to the momentum distribution $n_0(k)$ and to the total momentum distribution $n(k)$, respectively. In case of ^{3}He the dot-dashed, dashed, and long dashed lines correspond to Eq. (34) calculated in Ref. [20] at $E_f = 17.75, 55.5, 305.5$ MeV, whereas for nuclear matter the dot-dashed and dashed lines correspond [11] to $E_f = 100$ and 300 MeV, respectively.

decreasing at large k as powers of k, it has been argued that the nucleon spectral function at high values of both k and E should be governed by ground-state configurations in which the high-momentum $\vec{k}_1 \equiv \vec{k}$ of a nucleon is almost entirely balanced by the momentum $\vec{k}_2 \simeq -\vec{k}$ of another nucleon, with the remaining $(A-2)$ nucleons acting as a spectator with momentum $\vec{k}_{A-2} \simeq 0$.[2] When the momentum and the intrinsic excitation energy of the $(A-2)$ system are totally disregarded, the energy conservation would require that

$$E^*_{A-1} + E^R_{A-1} \simeq \frac{k^2}{2M}, \tag{35}$$

where $E^R_{A-1} = k^2/2(A-1)M$ is the recoil energy of the $(A-1)$-nucleon system; thus the intrinsic excitation of the $(A-1)$ system would be

$$E^*_{A-1} = \frac{A-2}{A-1}\frac{k^2}{2M}. \tag{36}$$

Within such a picture, the nucleon spectral function $P_1(k,E)$ has the following form:

$$P_1(k,E) = \frac{1}{4\pi} n_1(k)\, \delta[E - E_1^{(2\mathrm{NC})}(k)], \tag{37}$$

with

[2]Configurations corresponding to high values of $|\vec{k}_{A-2}|$ should be ascribed to three-nucleon correlations; indeed, high values of $|\vec{k}_{A-2}|$ can be due to ground-state configurations with a third "hard" nucleon, whose momentum balances the CM one of particles 1 and 2.

$$E_1^{(2\mathrm{NC})}(k)=E_{\mathrm{thr}}^{(2)}+\frac{A-2}{A-1}\frac{k^2}{2M}, \tag{38}$$

where $E_{\mathrm{thr}}^{(2)}\equiv|E_A|-|E_{A-2}|$ is the two-nucleon breakup threshold.

Let us denote by $E_1^{\mathrm{peak}}(k)$ the value of the removal energy at which, for a given momentum k, the spectral function $P_1(k,E)$ has its maximum, and by $\langle E(k)\rangle_1$ the mean removal energy for a given k, viz.

$$\langle E(k)\rangle_1\equiv\frac{4\pi}{n_1(k)}\int_{E_{\min}}^{\infty}dE\ EP_1(k,E). \tag{39}$$

Using the spectral function given by Eq. (37) one gets

$$\langle E(k)\rangle_1=E_1^{\mathrm{peak}}(k)=E_1^{(2\mathrm{NC})}(k). \tag{40}$$

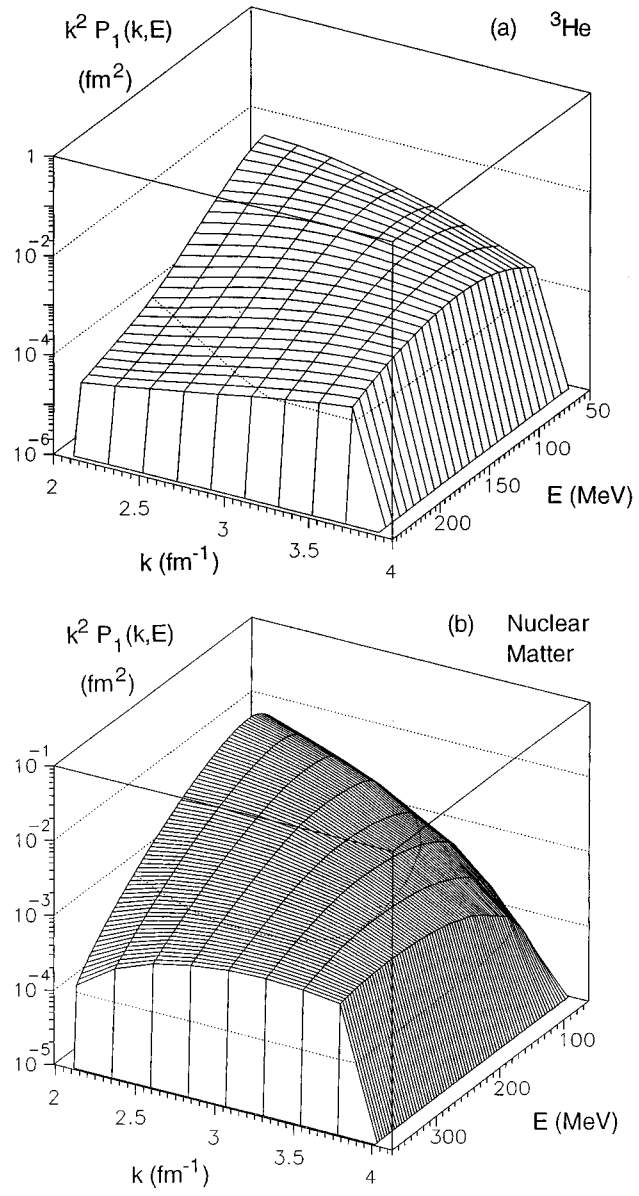

FIG. 4. Momentum and removal energy dependences of the nucleon spectral function $P(k,E)$ (times k^2) calculated in Ref. [10] for ^{3}He (a) and in Ref. [11] for infinite nuclear matter (b).

In what follows, the model given by Eq. (37) will be referred to as the two-nucleon correlation (2NC) model. At high values of k and E, the nucleon spectral function calculated in ^{3}He [10] and nuclear matter [11] exhibits, indeed, for fixed values of k, broad peaks in E, whose width increases with k. This is illustrated in Fig. 4, where the spectral function in ^{3}He and infinite nuclear matter are shown for $k>2$ fm^{-1} and $E>50$ MeV. In order to emphasize the high-momentum part of $P_1(k,E)$ due to NN correlations, the quantity $k^2\cdot P_1(k,E)$ has been plotted; it can indeed be seen that for fixed values of k, a peak-shaped behavior is exhibited, which can be characterized by three relevant quantities, viz. the peak position $E_1^{\mathrm{peak}}(k)$, the mean removal energy $\langle E(k)\rangle_1$ defined by Eq. (39) and the full width at half maximum (FWHM). In Ref. [1] a quantitative comparison between the 2NC model and the many-body spectral function has been presented. The results are reported in Fig. 5, which shows an impressive agreement between the value of $\langle E(k)\rangle_1$ calculated with the many-body spectral function and the predictions of the 2NC model. However, it can also be seen that the 2NC model cannot predict the difference between $\langle E(k)\rangle_1$ and $E_1^{\mathrm{peak}}(k)$ obtained within many-body calculations. Moreover, the 2NC model, by definition, cannot provide values of the spectral function for $E\neq E_1^{2NC}(k)$.

B. The extended two-nucleon correlation model

In Ref. [1] the NN correlation mechanism, which produces a nonvanishing spectral function for $E\neq E_1(k)$, has been found to be the motion of the CM of the correlated NN pair, and an expression of $P_1(k,E)$ in terms of a convolution integral of the relative and CM momentum distributions of a correlated pair has been derived in details for the case of ^{3}He. In this section we show that a convolution

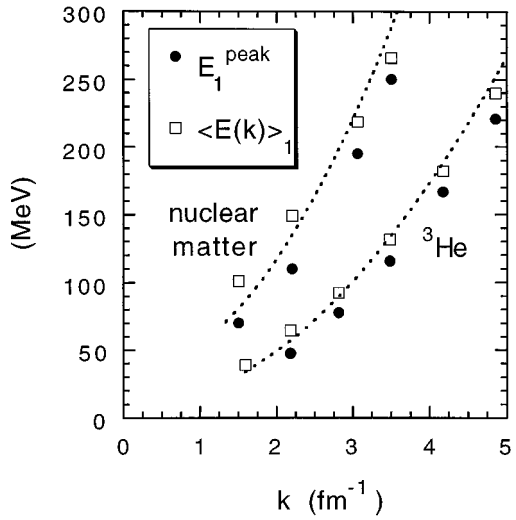

FIG. 5. Comparison of the values of the mean removal energy $\langle E(k)\rangle_1$ (open squares), defined by Eq. (39), and the peak position E_1^{peak} (full squares) for ^{3}He and nuclear matter, calculated with the spectral functions of Refs. [10] and [11], respectively, with the predictions of the 2NC model [see Eq. (37)]. The dotted lines are the results obtained using Eqs. (40) and (38), which yield explicitly $\langle E(k)\rangle_1=E_1^{\mathrm{peak}}=E_{\mathrm{thr}}^{(2)}+k^2/4M$ in case of ^{3}He and $\langle E(k)\rangle_1=E_1^{\mathrm{peak}}=E_{\mathrm{thr}}^{(2)}+k^2/2M$ for nuclear matter.

formula can be obtained for any value of the mass number A, and that such a convolution formula follows from the high $k-E$ limit of the spectral function. We will obtain our model of the spectral function of a nucleon N_1 ($N_1=n,p$) starting from the definition (4). We are interested in $2p$-$2h$ ($1p$-$2h$) configurations of Ψ_A^0 ($\Psi_{A-1}^{f_{A-1}}$) appearing in the overlap integral (3). The following Jacobian coordinates and conjugate momenta referring to particles 1 and 2 (with rest mass M) in the continuum, and "particle" 3 [the $(A-2)$-nucleon system] with rest mass $(A-2)M$, will be used

$$\vec{x}=\vec{r}_1-\vec{r}_2, \quad \vec{k}_x=\frac{\vec{k}_1-\vec{k}_2}{2}, \quad \vec{y}=\vec{r}_3-\frac{\vec{r}_1+\vec{r}_2}{2}$$

$$\vec{k}_y=\frac{2\vec{k}_3-(A-2)(\vec{k}_1+\vec{k}_2)}{A}. \tag{41}$$

In what follows the sets of coordinates $\{\vec{r}_i\}$ and conjugate momenta $\{\vec{k}_i\}$ are measured from the CM of the nucleus (i.e., they satisfy the relations $\Sigma_{i=1}^A \vec{r}_i=0$ and $\Sigma_{i=1}^A \vec{k}_i=0$), so that one has

$$\vec{k}_x=\frac{\vec{k}_1-\vec{k}_2}{2}\equiv\vec{k}_{\rm rel}, \quad \vec{k}_y=\vec{k}_3=-(\vec{k}_1+\vec{k}_2)\equiv-\vec{k}_{\rm CM}, \tag{42}$$

where $\vec{k}_{\rm rel}$ and $\vec{k}_{\rm CM}$ are the relative and CM momentum of the correlated NN pair, respectively. In terms of these variables the ground-state wave function can be written in the following general form:

$$\Psi_A^0(\{\vec{r}_i\}_A)=\hat{\mathscr{A}}_A\Big\{\sum_{nmf_{A-2}} a_{nmf_{A-2}}[\Phi_n(\vec{x})\otimes\chi_m(\vec{y})] \otimes\Psi_{A-2}^{f_{A-2}}(\{\vec{r}_i\}_{A-2})\Big\}, \tag{43}$$

where $\hat{\mathscr{A}}$ is a proper antisymmetrization operator; $\otimes$ is a short-hand notation for the standard Clebsh-Gordan coupling of orbital and spin angular momenta; $\{\Phi_n(\vec{x})\}$ ($\{\chi_m(\vec{y})\}$) represents a complete set of states describing the relative (CM) motion of the pair (1,2) and $\{\Psi_{A-2}^{f_{A-2}}(\{\vec{r}_i\}_{A-2})\}$ the complete set of states describing the $(A-2)$ system. The ansatz (43) is the exact one needed to calculate the spectral function corresponding to states in which two particles are in the continuum. Our aim, however, is to describe the high momentum and high removal energy parts of the spectral function. To this end, we adhere to the argument that such a part of $P_1(k,E)$ is generated by ground-state configurations in which two particles are strongly correlated, with the $(A-2)$ particles simply creating the mean field in which the correlated pair is moving. If we view such a configuration in momentum space, we would say that we are dealing with a NN correlated pair with a very high relative momentum ($|\vec{k}_x|>k_f\sim1.5$ fm^{-1}) and a low CM momentum ($|\vec{k}_y|<1.5$ fm^{-1}); these assumptions allows one to safely describe the CM motion wave function in (43) by an s-wave state (which we denote by $m=0$), obtaining

$$\Psi_A^0(\{\vec{r}_i\}_A)\simeq\hat{\mathscr{A}}\Big\{\chi_0(\vec{y})\sum_{nf_{A-2}} a_{n0f_{A-2}}[\Phi_n(\vec{x}) \otimes\Psi_{A-2}^{f_{A-2}}(\{\vec{r}_i\}_{A-2})]\Big\}. \tag{44}$$

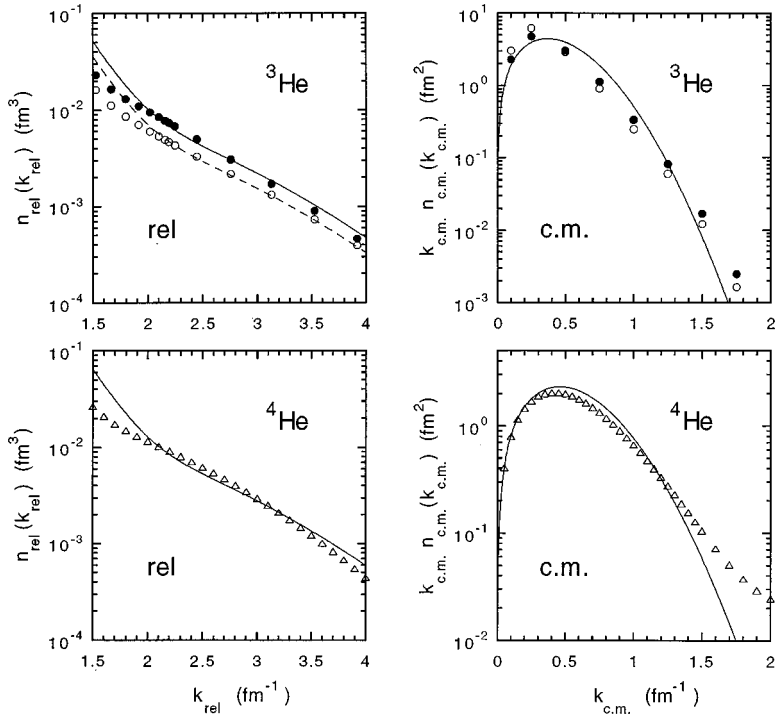

FIG. 6. The high-momentum part of the relative (rel) momentum distribution and the low-momentum part of center-of-mass (CM) momentum distribution [see Eq. (42) for the definition of the relative and CM momenta of a correlated NN pair). In case of ^{3}He the open (full) dots correspond to the results of Refs. [10] and [9], for a pp (nn) pair, respectively (the interaction is the RSC one [30]); the full and dashed lines for $n_{\rm rel}$ represent the rescaled deuteron momentum distributions [Eq. (55) with $C^A=1.8$ for the pp pair and $C^A=2.5$ for the pn pair], whereas the full line for $n_{\rm CM}$ is the Gaussian parametrization given by Eq. (56). In case of ^{4}He the triangles represent the results obtained in Ref. [21] using the RSC interaction, whereas the full curves are the rescaled deuteron momentum distribution for $n_{\rm rel}$ [Eq. (55) with $C^A=3.2$] and the Gaussian parametrization of Eq. (56) for $n_{\rm CM}$. The values adopted for the parameter $\alpha_{\rm CM}$ are reported in Table I.

To further elaborate on the structure of the wave function (44), we make use of the results illustrated in Sec. II C, namely, since the CM of the pair involves only low-momentum components, the excitation spectrum of the $(A-2)$ system ($\{f_{A-2}\}$) is mainly limited to the ground state and to the (low-lying) excited states corresponding to configurations generated by the removal of two particles from different shell model states of the target; thus denoting such states by $f_{A-2}=\bar{0}$, we have

$$\Psi_A^0(\{\vec{r}_i\}_A)\simeq\hat{\mathscr{A}}\{\chi_0(\vec{y})[\Phi(\vec{x})\otimes\Psi_{A-2}^{\bar{0}}(\{\vec{r}_i\}_{A-2})]\}, \quad (45)$$

where

$$\Phi(\vec{x})=\sum_n a_{n\bar{0}0}\Phi_n(\vec{x}) \quad (46)$$

describes the relative motion of the correlated pair in the nuclear medium, which at small $|\vec{x}|$ can be considered independent of the particular shells from which the two nucleons of the pair are removed by the effects of short-range NN correlations. Let us reiterate that Eq. (45) is our basic starting point for obtaining the spectral function. The basic assumption underlying Eq. (45) is that high-momentum components in nuclei are due to strong correlations between two nucleons, whose CM momentum is a low one (which, in turns, means that $|\vec{x}|<<|\vec{y}|$); once such an assumption is made, it follows that the $(A-2)$ system is in its ground state; the nucleons belonging to the $(A-2)$ ''spectator'' system may well be strongly correlated between themselves, but the basic assumption is that they are almost independent from the ''active'' correlated pair which ''feels'' the $(A-2)$ system only through the low-momentum CM motion. An important feature of our 2NC model is that high values of the excitation energy of the residual $(A-1)$ system are almost totally due to high values of the kinetic energy of the relative motion of the correlated nucleon with the ''spectator'' $(A-2)$ system, i.e., they are not generated by high values of the excitation energy of the $(A-2)$ system. To sum up, we assume that the ansatz (45) can describe the real configurations leading to the high momentum and high removal energy components of the spectral function.

Let us now discuss the final states $\Psi_{A-1}^{f_{A-1}}$ of the residual $(A-1)$-nucleon system. The wave function $\Psi_{A-1}^{f_{A-1}}$ is approximated as

$$\Psi_{A-1}^{f_{A-1}}(\{\vec{r}_i\}_{A-1})=\hat{\mathscr{A}}_{A-1}\{e^{i\vec{k}_2\cdot\vec{r}_2}\otimes\Psi_{A-2}^{\tilde{f}_{A-2}}(\{\vec{r}_i\}_{A-2})\}, \quad (47)$$

where the distortion effects arising from the rescattering of particle 2 with ''particle 3'' have been neglected. The form (48) is the natural extension to the final states of the residual system of the basic assumption underlying Eq. (44) for the initial state. As a matter of fact, after the removal of particle 1 from a correlated pair, the correlated particle 2 is emitted because of recoil and ''feels'' the mean field produced by the $(A-2)$ system only in the low-momentum part of its final amplitude. In other words, the final state interaction of particle 2 is suppressed by the fact that the configurations relevant for the high k-E part of the nucleon spectral function are those in which $|\vec{x}|\ll|\vec{y}|$. It should be pointed out that in case of ^{3}He explicit many-body calculations [39] of the nucleon spectral function clearly show that the effects of the interaction in the residual system are relevant only for the low removal-energy part of $P_1(k,E)$, whereas they are negligible for the high k-E component which we are interested in.

Placing Eqs. (45) and (47) into Eq. (3) and omitting spin indices for sake of simplicity, we get for the Fourier transform of the overlap integral the following expression:

$$\int d\vec{z}\; e^{i\vec{k}\cdot\vec{z}}G_{f0}(\vec{z})\propto\int d\vec{x}\; d\vec{y}\; e^{i\vec{k}_x\cdot\vec{x}+i\vec{k}_y\cdot\vec{y}}\chi_0(\vec{y})\Phi(\vec{x})$$
$$=\tilde{\chi}_0(\vec{k}_y)\tilde{\Phi}(\vec{k}_x), \quad (48)$$

where $\tilde{\Phi}(\vec{k}_x)$ $[\tilde{\chi}_0(\vec{k}_y)]$ is the amplitude for the relative (CM) motion of the correlated pair in momentum space. Within our model the energy conservation appearing in Eq. (4) reads as follows:

$$E-E_{A-1}^f+E_A=E+|E_{A-2}|-\frac{|\vec{t}|^2}{2\mu}-|E_A|$$
$$=E-\left(E_{\rm thr}^{(2)}+\frac{|\vec{t}|^2}{2\mu}\right), \quad (49)$$

where

$$\frac{|\vec{t}|^2}{2\mu}\equiv\frac{(A-1)}{2M(A-2)}\left[\frac{(A-2)\vec{k}_2-\vec{k}_3}{A-1}\right]^2$$
$$=\frac{(A-2)}{2M(A-1)}\left[\vec{k}+\frac{(A-1)\vec{k}_3}{A-2}\right]^2 \quad (50)$$

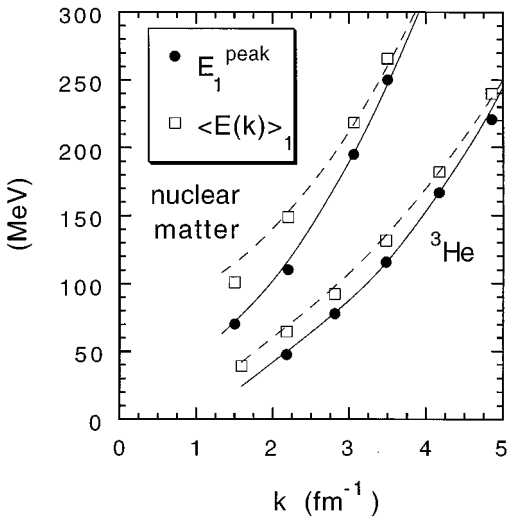

FIG. 7. Comparison of the values of the mean removal energy $\langle E(k)\rangle_1$ (open squares), defined by Eq. (39), and the peak position $E_1^{\rm peak}$ (full squares) for ^{3}He and nuclear matter, calculated with the spectral functions of Refs. [10] and [11], respectively, with the predictions of the extended 2NC model [see Eq. (51)]. The dashed and solid lines correspond, respectively, to the values of $\langle E(k)\rangle_1$ and $E_1^{\rm peak}$ obtained using in Eq. (53) the effective relative and CM momentum distributions given by Eqs. (55) and (56), respectively.

is the energy of the relative motion of particle 2 and "3" $(A-2)$, i.e., the excitation energy of the $(A-1)$ system. Thus placing Eqs. (48)–(50) into Eq. (4) the following convolution formula is obtained for any value of A:

$$P_1^{(N_1)}(k,E)=\mathcal{N}\sum_{N_2=n,p}\int d\vec{k}_3\ \delta\Bigg[E-E_{\rm thr}^{(2)}-\frac{(A-2)}{2M(A-1)}\times\left(\vec{k}+\frac{(A-1)\vec{k}_3}{(A-2)}\right)^2\Bigg]n_{\rm rel}^{N_1N_2}\left(\left|\vec{k}+\frac{\vec{k}_3}{2}\right|\right)\times n_{\rm CM}^{N_1N_2}(|\vec{k}_3|). \quad (51)$$

In Eq. (51) the value of $\mathcal{N}$ can be chosen in order to reproduce the correlated part of the nucleon momentum distribution $n_1(k)=n(k)-n_0(k)[\simeq n(k)$ for $k>1.5$ fm$^{-1}]$, viz.

$$\int_{E_{\rm thr}^{(2)}}^{\infty}dE\ P_1^{(N_1)}(k,E)=n_1(k). \quad (52)$$

From Eq. (51) it can be seen that the $2NC$ model can be recovered by placing $n_{\rm CM}^{N_1N_2}(\vec{k}_3)=\delta(\vec{k}_3)$, i.e., the spectator nucleon at rest. When the motion of the latter and the link between $\vec{k}$, $\vec{k}_3$ and E are considered, a nucleon spectral function in the whole range of variation of E $(E_{\rm thr}^{(2)}\leqslant E<\infty)$ is generated. Moreover, the removal energy dependence of $P_1^{(N_1)}(k,E)$ is governed by the behavior of $n_{\rm CM}^{N_1N_2}$ and $n_{\rm rel}^{N_1N_2}$, whose calculation, unlike the case of the spectral function itself, requires the knowledge of the ground-state wave function only.

A further integration in Eq. (51) over the angular variables of $\vec{k}_3$ yields

$$P_1^{(N_1)}(k,E)=\frac{2\pi M}{k}\mathcal{N}\sum_{N_2=n,p}\int_{k_3^-}^{k_3^+}dk_3\ k_3 n_{\rm rel}^{N_1N_2}(k_x^*)n_{\rm CM}^{N_1N_2}(k_3), \quad (53)$$

where $k_3\equiv|\vec{k}_3|$ and

$$k_3^{\pm}=\frac{A-2}{A-1}|k\pm k_0|,\quad k_0=\sqrt{2M\frac{A-1}{A-2}[E-E_{\rm thr}^{(2)}]},$$

$$k_x^*=\sqrt{\frac{Ak^2+(A-2)k_0^2}{2(A-1)}-\frac{Ak_3^2}{4(A-2)}}. \quad (54)$$

It can be easily seen that Eq. (53) reduces for $A=3$ to the convolution formula given by Eq. (18) of Ref. [1]. As already pointed out, in Eq. (53) $n_{\rm rel}^{N_1N_2}$ refers to a proper spin and isospin combination of a N_1N_2 pair in the continuum, and, correspondingly, $n_{\rm CM}^{N_1N_2}$ represents the momentum distribution of a N_1N_2 pair with respect to the $(A-2)$ system in its ground state. The "three-body" configuration underlying Eq. (53) is such that two correlated particles are very close, whereas the $(A-2)$ core is far from their CM. Therefore, in Eq. (53) the relevant contribution has to be provided by the low-momentum part of $n_{\rm CM}^{N_1N_2}$ and by the high-momentum one of $n_{\rm rel}^{N_1N_2}$. Such a ground-state configuration is automatically generated by the use of the CM momentum distribution in the $\ell=0$ (mean field) state, which, for $k>2$ fm^{-1}, does not include the high-momentum components generated by the short-range and tensor correlations. We would like to stress here that, according to our assumptions, Eq. (53) is expected to correctly describe the nucleon spectral function only for high values of k and E, when the $(A-2)$ system is in its ground state; in terms of $n_{\rm rel}^{N_1N_2}$ and $n_{\rm CM}^{N_1N_2}$ it means that only high (low) values of k_x^* (k_3) have to be considered in Eq. (53).

IV. THE MODEL SPECTRAL FUNCTION FOR FEW-NUCLEON SYSTEMS AND COMPLEX NUCLEI

In this section our model spectral function will be presented for $3\leqslant A<\infty$. For the three-nucleon system and infinite nuclear matter our model spectral function will be compared with the one obtained from many-body calculations. According to Eq. (53), the basic ingredients to calculate the spectral function are the relative and CM momentum distributions of NN pair in the nucleus. These quantities have been calculated for $A=3,4$ and their behavior will be discussed together with model distributions for complex nuclei.

A. The relative and CM momentum distributions

The quantities (30) and (31) pertaining to a neutron-proton and neutron (proton)–neutron (proton) pairs in ^{3}He and ^{4}He, calculated in Refs. [10] and [36] using the Reid soft core interaction [30], are presented in Fig. 6, where they are compared with a rescaled deuteron momentum distribution for the high-momentum part of the relative distributions and with a simple Gaussian parametrization for the low-momentum part of the CM distributions [see also Eq. (42) which relates the relative and CM momenta ($\vec{k}_{\rm rel}$ and $\vec{k}_{\rm CM}$) with the Jacobian momenta $\vec{k}_x$ and $\vec{k}_3$ appearing in Eq. (53)]. It can be seen that (i) the high-momentum part of the relative distribution can be very accurately explained by a rescaled deuteron momentum distribution, as suggested by several investigations; therefore, the following effective relative momentum distribution will be used in Eq. (53)

$$n_{\rm rel}^{\rm eff}(k_{\rm rel})=C^A n_D(k_{\rm rel}), \quad (55)$$

where C^A is the same constant appearing in Eq. (29);[3] (ii) the low-momentum part of $n_{\rm CM}^{N_1N_2}$ can be fairly well reproduced by a Gaussian distribution, in agreement with our assumption that the CM moves in an s-wave state; thus, for complex nuclei we will use in Eq. (53) the following effective CM momentum distribution:

$$n_{\rm CM}^{\rm eff}(k_{\rm CM})=\left(\frac{\alpha_{\rm CM}}{\pi}\right)^{3/2}e^{-\alpha_{\rm CM}k_{\rm CM}^2} \quad (56)$$

with the parameter $\alpha_{\rm CM}$ determined as follows. Let us start from the trivial relation $\langle(\Sigma_{i=1}^A\vec{k}_i)^2\rangle=0$, where the expectation value is performed with respect to the intrinsic wave

[3]Note that by using (55) in (51) one gets, due to (29), that $\mathcal{N}\simeq 1$ for $k>2$ fm^{-1}.

TABLE I. The values of the parameters C^A [Eq. (55)] and $\alpha_{\rm CM}$ [Eq. (56)] for various nuclei. The value of C^A is estimated from the height of the plateau exhibited by the ratio of the nucleon momentum distribution $n(k)$ of a nucleus to the one of the deuteron at $k>2$ fm^{-1} [see Fig. 2(b)]. The value of $\alpha_{\rm CM}$ is calculated using Eq. (57). In case of ^{3}He and ^{4}He the value of $\langle T\rangle^{(\rm SM)}$ is estimated adopting a simple harmonic oscillator (HO) wave function with the value of the HO length chosen in order to reproduce the experimental value of the charge radius of the nucleus. In case of $A=\infty$ the Fermi-gas prediction (i.e., $\langle T\rangle^{(\rm FG)}=3k_F^2/10M$) is considered with $k_F=1.33$ fm^{-1}.

Nucleus	C^A	$\langle T\rangle^{(\rm SM)}$ (MeV)	$\alpha_{\rm CM}$ (fm^2)
^{3}He	1.9	8.5	3.7
^{4}He	3.8	9.8	2.4
^{12}C	4.0	16.9	1.0
^{16}O	4.2	14.0	1.2
^{40}Ca	4.4	16.7	0.98
^{56}Fe	4.5	14.3	1.1
^{208}Pb	4.8	18.4	0.85
$A=\infty$	4.9	22.0	0.71

function Ψ_A^0; such a relation implies $A\langle k^2\rangle+A(A-1)\langle\vec{k}_1\cdot\vec{k}_2\rangle=0$, where $\langle k^2\rangle$ is the mean value of the squared single nucleon momentum; then $\langle k_{\rm CM}^2\rangle=2(A-2)\langle k^2\rangle/(A-1)$. Since, according to our model, the distribution (56) should not include high-momentum components generated by short-range and tensor correlations, the value of $\langle k^2\rangle$ is taken to be equal to the one obtained within the mean-field approach. Therefore, $\alpha_{\rm CM}$ appearing in Eq. (56) is given by

$$\alpha_{\rm CM}=\frac{3}{2\langle k_{\rm CM}^2\rangle}=\frac{3(A-1)}{4(A-2)}\frac{1}{2M\langle T\rangle^{(\rm SM)}}, \tag{57}$$

where $\langle T\rangle^{(\rm SM)}$ is the expectation value of the (single) nucleon kinetic energy calculated within the mean-field approach. The value of $\alpha_{\rm CM}$ determined by Eq. (57) for various nuclei as well as the value of the parameter C^A Appearing in Eq. (55) are listed in Table I.

B. The nucleon spectral function of ^{3}He and nuclear matter

Here, the quantity $P_1(k,E)$ for ^{3}He and infinite nuclear matter calculated from Eq. (53) will be presented and compared with the same quantity calculated from many-body approaches already discussed and shown in Fig. 4. First of all, let us show the comparison between our model predictions for the peak position $E_1^{\rm peak}(k)$, the mean removal energy $_1$ and the FWHM, with the predictions from many-body calculations. An inspection at Eq. (53) shows qualitatively the following relevant features of the spectral function: (i) if $n_{\rm rel}$ and $n_{\rm CM}$ are described within an independent particle model (e.g., Gaussians with the same length parameter), Eq. (53) predicts a maximum of the spectral function close to $E=E_{\rm thr}^{(2)}$ with a monotonic decrease with E; (ii) because of the k_3 and k_0 dependence of the argument k_x^* of $n_{\rm rel}$, the spectral function exhibits a peak-shaped behavior with the peak position located at a value lower than the one predicted by the 2NC model [see Eq. (38)]; (iii) the shift of the peak position with respect to the 2NC model, as well as the shape of the spectral function near the peak, are mostly governed by the high k_0 dependence of $n_{\rm rel}(k_x^*)$. If the latter is chosen to be of the Gaussian form, the peak position and the FWHM can be expressed as a series expansion in terms of the parameter

$$\gamma\equiv\frac{A-1}{2(A-2)}\langle k_{\rm CM}^2\rangle/\langle k_{\rm rel}^2\rangle, \tag{58}$$

where $\langle k_{\rm rel}^2\rangle$ and $\langle k_{\rm CM}^2\rangle$ are the mean-square momenta associated to the high and the low-momentum parts of $n_{\rm rel}$ and $n_{\rm CM}$, respectively. One has

$$E_1^{\rm peak}(k)\simeq E_{\rm thr}^{(2)}+\frac{A-2}{A-1}\frac{k^2}{2M}[1-2\gamma]+O(\gamma^2), \tag{59}$$

$$\mathrm{FWHM}(k)\simeq\sqrt{\frac{\langle k_{\rm CM}^2\rangle 8\ \ln 2}{3}}(1-\gamma)\frac{k}{M}+O(\gamma^2). \tag{60}$$

Equations (59) and (60) show again that in the limit of a static spectator $(A-2)$ system (i.e., $\langle k_{\rm CM}^2\rangle\to 0$) the 2NC model is recovered [i.e., $E_1^{\rm peak}(k)=E_{\rm thr}^{(2)}+(A-2)k^2/2(A-1)M$ and FWHM = 0]. The motion of the spectator system, coupled, through energy and momentum conservation, to the relative motion of the correlated pair [cf. Eq. (53)], produces both a shift (by a percentage amount of the order of $\simeq 2\gamma$) of the peak position from the value predicted by the 2NC model, as well as the removal energy dependence of the spectral function for $E\neq E_1^{\rm peak}(k)$. The validity of the above expressions relies on the smallness of the parameter γ. From many-body calculations [9–11] one gets $\langle k_{\rm rel}^2\rangle\sim 6$ fm^{-2} (~ 7 fm^{-2}) and $\langle k_{\rm CM}^2\rangle\sim 0.5$ fm^{-2} (~ 2 fm^{-2}) for ^{3}He (nuclear matter), so that $\gamma_{^3\rm He}\sim 0.08$ ($\gamma_{\rm NM}\sim 0.14$). In Figs. 8 and 9 $E_1^{\rm peak}(k)$ and FWHM calculated using Eqs. (59) and (60), as well as using the full spectral function, are compared with the corresponding quantities predicted by many-body spectral functions shown in Fig. 4. It can be seen that (i) unlike the 2NC model in which $\langle E(k)\rangle_1=E_1^{\rm peak}(k)$, in disagreement with the results of theoretical calculations, Eq. (53) is able to correctly predict the relation $\langle E(k)\rangle_1>E_1^{\rm peak}(k)$ (cf. Fig. 7); (ii) the values of the FWHM, which is obviously zero in the 2NC model, is correctly predicted by Eq. (53). It turns out also that from the results presented in Fig. 8, the linear dependence of the FWHM upon k [see Eq. (60)] provides a satisfactory reproduction of the average value of the FWHM up to large value of k; at the same time, it appears that the calculations with the many-body spectral function also give rise to terms quadratic in k, which are reproduced by evaluating Eq. (53) with realistic momentum distributions. Eventually, in Fig. 9 we present a direct comparison of our model spectral function with the many-body ones. It can be seen that the whole shape of $P_1(k,E)$ is satisfactorily reproduced in a wide range of values of E around the peak. It can be noticed that the range of k and E for which our model can be applied is wider in nuclear matter than in ^{3}He. This is a typical A-dependent effect, since it is due to the A dependence of the FWHM [cf. Eq. (60)]. In Fig. 10 we provide a three-dimensional plot of the spectral functions; there it can be seen that, whereas for

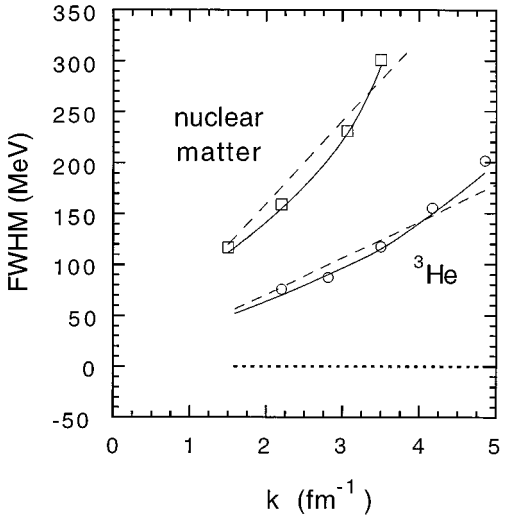

FIG. 8. Comparison of the values of the full width at half maximum (FWHM) calculated using the spectral functions of Refs. [10] for ^{3}He (open dots) and [11] for nuclear matter (open squares), with the predictions of the extended 2NC model [see Eq. (51)]. The dashed line corresponds to the predictions of Eq. (60), whereas the solid line is the results obtained using our model spectral function, calculated using in Eq. (53) the effective relative and CM momentum distributions given by Eqs. (55) and (56), respectively. The dotted line represents the prediction of the ''naive'' 2NC model [see Eq. (37), in which the CM of the correlated pair is assumed to be at rest].

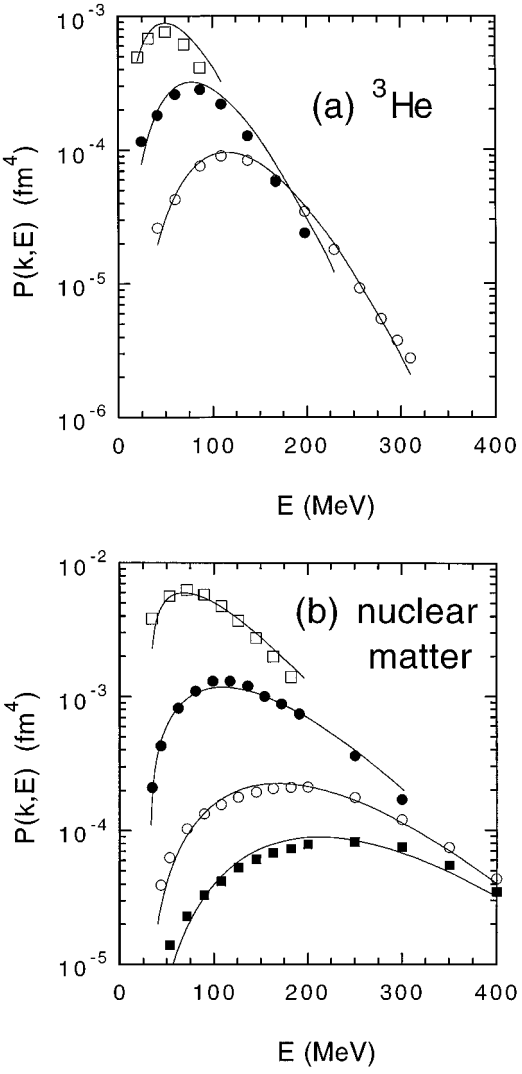

FIG. 9. The nucleon spectral function of ^{3}He [10] and nuclear matter [11] versus the removal energy E for various values of the nucleon momentum. For ^{3}He (a) the squares, full dots, and open dots correspond to $k=2.2$, 2.8, and 3.5 fm^{-1}, respectively. For nuclear matter (b) the open squares, full dots, open dots, and full squares correspond to $k=1.5$, 2.2, 3.0, and 3.5 fm^{-1}, respectively. The solid lines are the predictions of our extended 2NC model obtained using in Eq. (53) the effective relative and CM momentum distributions given by Eqs. (55) and (56). The value of the constant $\mathcal{N}$ appearing in Eq. (51) is fixed by Eq. (52), in which the correlated part $n_1(k)$ of the nucleon momentum distribution calculated in Refs. [10] and [11] has been used.

nuclear matter the agreement between the model and many-body spectral functions is a satisfactory one in the whole range of momenta and energies considered, in ^{3}He an appreciable disagreement in the low k–high E region can be observed. Such a disagreement, which, we reiterate, appears in ^{3}He but not in nuclear matter, can be ascribed to the effects of three and more nucleon correlations for the following reason: our model includes two-nucleon correlations only, i.e., it cannot account for three and more nucleon correlations, which correspond to configurations in which more than two particles get close by. Since the ''exact'' ^{3}He spectral function includes three-nucleon correlations, and since these mainly affect very low and very high energy tails, the reason for the disagreement in ^{3}He is clear: it is due to the absence of three-nucleon correlations in our model. On the other hand side, in the case of nuclear matter, the overall agreement between the many-body [11] and our model spectral functions would probably indicate that the three-nucleon correlations, generated by the Jastrow correlation factor in Ref. [11], do not produce a sizable effect on $P(k,E)$, at least in the $k-E$ region considered. Thus we can conclude that our model spectral function describes correctly the $k-E$ dependence of the real spectral function generated by two-nucleon correlations in the range $k>2$ fm^{-1} and $E_L<E<E_1^{\rm peak}(k)$ $+\mathrm{FWHM}(k)$, where $E_1^{\rm peak}(k)$ and the FWHM can be safely estimated by Eqs. (59) and (60). From Fig. 9 the value of E_L can be estimated to be $\sim 30-50$ MeV, depending on the momentum k. Moreover, we would like to point out that, using Eq. (54), the lower limit of integration k_3^- in Eq. (53), calculated at $E=E_1^{\rm peak}(k)+\mathrm{FWHM}(k)$, is less than 0.5 (1) fm^{-1} in ^{3}He (nuclear matter) and the corresponding value of the relative momentum k_x^* is greater than 2 fm^{-1}.

C. The nucleon spectral function of ^{4}He and multiparticle final states

To describe the spectral function for $A=4$ our model has to be implemented to take into account the so-called four-body channel, i.e., the configurations of the $(A-1)$ system with 3 particles in the continuum. The reason is as follows. The basic idea, leading to the convolution integral (51), was the assumption that $2p$-$2h$ ground-state correlations [cf. Eq.

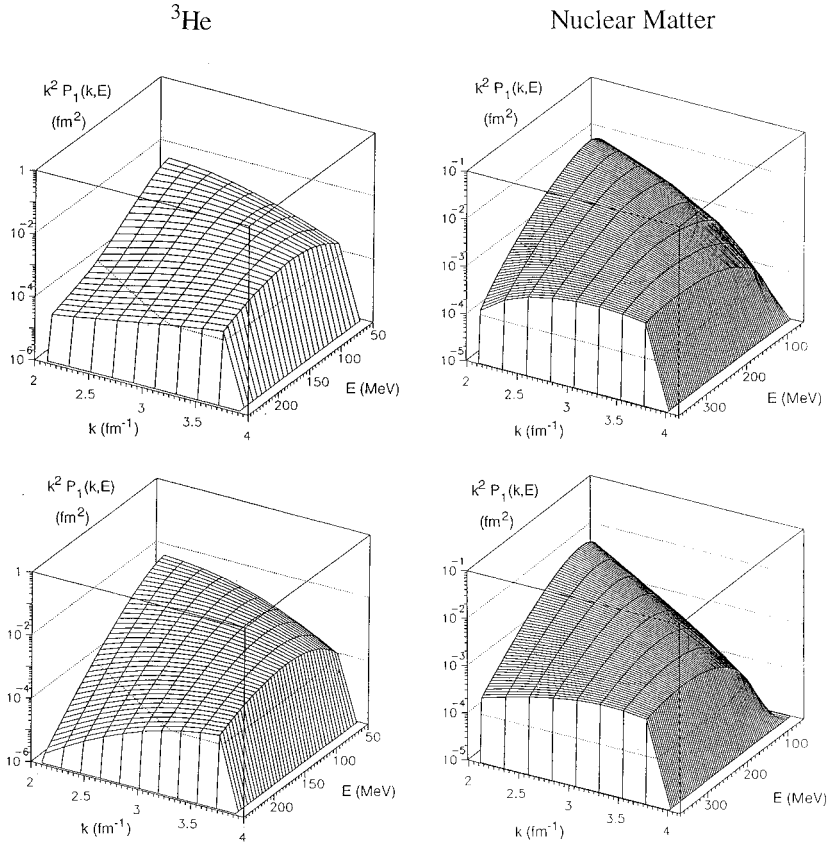

FIG. 10. Momentum and removal energy dependences of the nucleon spectral function $P(k,E)$ (times k^2) for $A=3$ (left side) and $A=\infty$ (right side). The predictions of our extended 2NC model, obtained using in Eq. (53) the effective relative and CM momentum distributions given by Eqs. (55) and (56), are shown in the lower part of the figure, whereas the results of the many-body calculations of Refs. [10] and [11] are shown in the upper one.

(44)] leading to $1p$-$2h$ states of the residual $(A-1)$ system [cf. Eq. (47)], are due, at high values of k and E, to configurations in which the high momentum of particle 1 is almost entirely balanced by the one of particle 2 with the ''third'' spectator particle [the $(A-2)$ system] far apart from the two correlated particles. The excitation energy of the $(A-1)$ system corresponding to such a configuration is mainly due (particularly around the peak where $\vec{k}_2 \simeq -\vec{k}$ and $|\vec{k}_3| \sim 0$) to the kinetic energy of the relative motion of particles 2 and 3, with the latter [the $(A-2)$ system] being, as previously explained, in low-lying excited states. When $E > E_1^{\rm peak}(k)$ one has $\vec{k}_2 \neq -\vec{k}$ and, in particular, one can have $|\vec{k}_2| < |\vec{k}|$, if high values of the excitation energy of the $(A-2)$ system are allowed. Such a mechanism is absent in our model, which effectively takes into account only $2p$-$2h$ ground-state correlations and, as already pointed out, the agreement we found with the many-body calculations of nuclear matter makes us confident of the correctness of our approach. To sum up, in a complex nucleus the removal energy behavior of the spectral function at high values of k is determined only by the relative motion of particles 2 and 3. In ^{4}He the situation appears to be rather different, for the $(A-2)$ system is the weakly bound deuteron. Thus, for fixed values of E even a small difference between $|\vec{k}_2|$ and $|\vec{k}|$ at the peak can originate an intrinsic excitation of the residual $(A-2)$ system, which is sufficient to break up the deuteron giving rise to the four-body channel. In other words, our model represented by Eq. (51) with the hard part of $n_{\rm rel}$, cannot be applied to the calculation of the two-nucleon emission channel, for considering $n_{\rm rel}^{\rm hard}$ will unavoidably lead to a break up of the residual deuteron. Moreover, it should be reminded that only in the case of a neutron-proton pair (with total isospin equal to 0) the residual system can be a deuteron, whereas for other types of correlated NN pairs the $(A-2)$ system can be only in the continuum. Therefore we have to describe, within our model, the four-body channel. This can easily be done by the following steps: (i) the summation over f_{A-2} has to be kept in Eq. (44); (ii) the factorization of the relative motion of the pair and the intrinsic excitation of the $(A-2)$ system is assumed to hold. The final result is

$$P_1^{(N_1)}(k,E) = \mathcal{N}(k) \sum_{N_2=n,p} \int d\vec{k}_3 \; n_{\rm rel}^{N_1N_2}\left(\left|\vec{k}+\frac{\vec{k}_3}{2}\right|\right) \times n_{\rm CM}^{N_1N_2}(|\vec{k}_3|) \cdot \int d\vec{t} \; w(|\vec{t}|)\, \delta\left[E - \frac{t^2}{M} - \frac{1}{3M} \times \left(\vec{k}+\frac{3\vec{k}_3}{2}\right)^2\right], \tag{61}$$

where $w(|\vec{t}|)$ represents the probability distribution to have a two-nucleon final state with excitation energy t^2/M. We have evaluated Eq. (61) by replacing $w(|\vec{t}|)$ with the hard part of the deuteron momentum distribution; the results are presented in Fig. 11 in correspondence of different values of the upper limit of integration over $|\vec{t}| = \sqrt{M E^*_{A-2}}$. In the same figure the results of the contribution of the four-body channel calculated in Ref. [17] are also shown.

D. The nucleon spectral function for complex nuclei

Given the success of our model for ^{3}He, ^{4}He and nuclear matter we are confident that it can safely be applied to com-

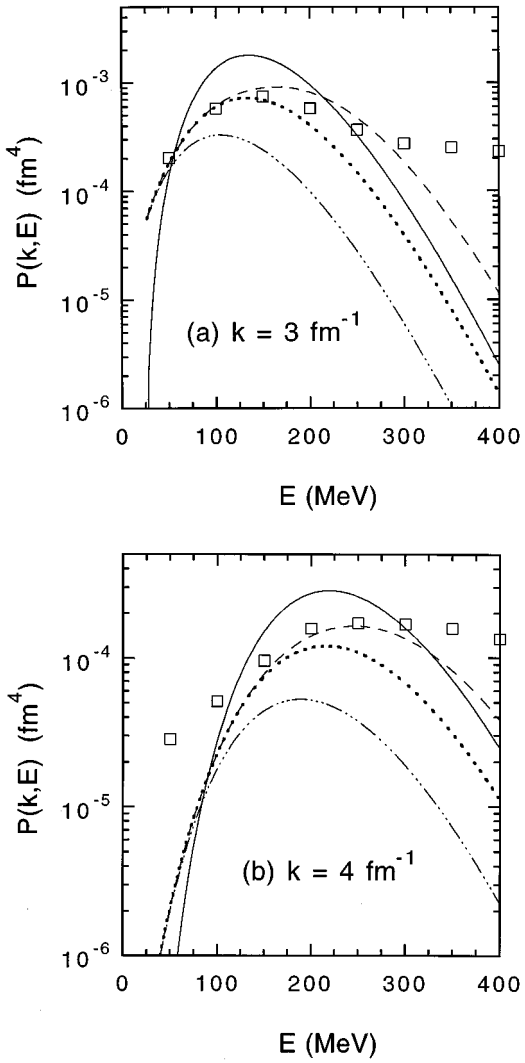

FIG. 11. The nucleon spectral function of ^{4}He [17] versus the removal energy E for two values of the nucleon momentum: $k=3$ fm^{-1} (a) and $k=4$ fm^{-1} (b). The open squares are the results of the many-body calculations of Ref. [17], whereas the solid lines are the predictions of Eq. (53) using the effective relative and CM momentum distributions given by Eqs. (55) and (56). The dot-dashed, dotted, and dashed lines are the results of Eq. (61) obtained using for $w(|\vec{t}|)$ the hard part of the deuteron momentum distribution and adopting the values 1.0, 1.5, and 2.0 fm^{-1}, respectively, for the upper limit of integration over $|\vec{t}|=\sqrt{ME_2^*}$, with E_2^* being the (positive) excitation energy of the residual two-nucleon system.

plex nuclei. In Fig. 12 we present the spectral function for ^{16}O; the results for other complex nuclei look very similar. In Fig. 13 we show the saturation of the energy and momentum sum rules, i.e., the quantities

$$S_f(E)=4\pi\int_0^{k_f} dk\ k^2P(k,E) \tag{62}$$

and

$$n_f(k)=4\pi\int_{E_{\min}}^{E_f} dE\ P(k,E). \tag{63}$$

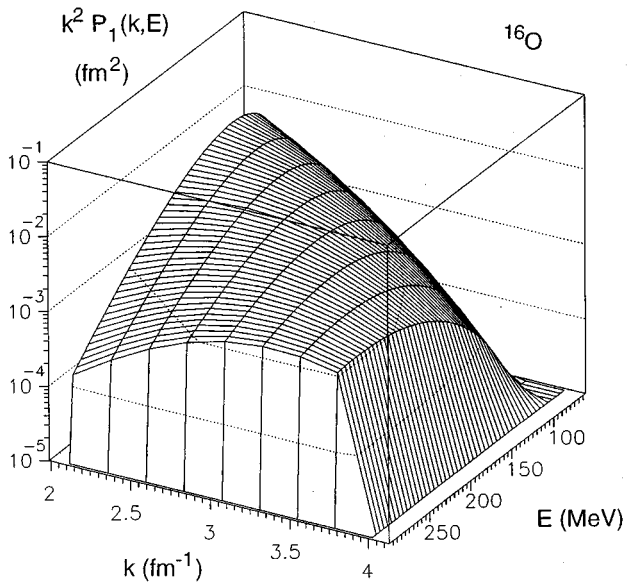

FIG. 12. Momentum and removal energy dependences of the nucleon spectral function $P(k,E)$ (times k^2) predicted by our extended 2NC model for ^{16}O using in Eq. (53) the effective relative and CM momentum distributions given by Eqs. (55) and (56).

As far as the latter quantity is concerned, the trend found for ^{3}He and nuclear matter (see Sec. II D) is confirmed (see Fig. 3); as for the former one, it can be seen that in order to saturate the energy sum rule, momentum components larger than 2 fm^{-1} are necessary.

Another quantity of interest is the energy-weighted sum rule [40]

$$\varepsilon_A=\frac{1}{M}\left[\frac{A-2}{A-1}\langle T\rangle-\langle E\rangle\right], \tag{64}$$

which relates the total binding energy per particle (ε_A) to the mean value of the nucleon removal energy

$$\langle E\rangle=\int d\vec{k}\ dE\ EP(k,E) \tag{65}$$

and of the nucleon kinetic energy

$$\langle T\rangle=\int_0^\infty dk\ k^2\frac{k^2}{2M}n(k). \tag{66}$$

Using Eq. (12) for $P_0(k,E)$ and our extended 2NC model for $P_1(k,E)$ the mean removal energy has been calculated for several complex nuclei. In Table II our results are reported and compared with those obtained using in Eq. (64) the experimental values of ε_A and the values of $\langle T\rangle$ calculated using Eq. (66) the nucleon momentum distribution $n(k)$ obtained within many-body approaches. It can be seen that our model spectral function satisfies the energy-weighted sum rule (64).

Recently [41] a model spectral function for complex nuclei, based on the application of the local density approximation (LDA) to the correlated part $P_1(k,E)$, has been proposed. A direct comparison between the two approaches cannot be performed, since the behavior of the spectral func-

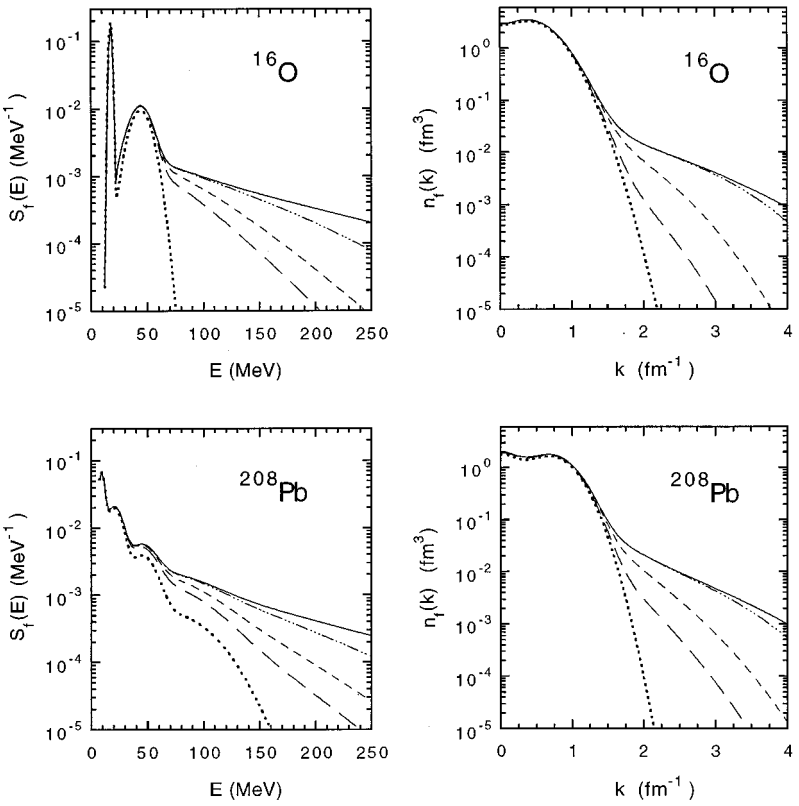

FIG. 13. The saturation of the energy $[S_f(E)$, (62)] and momentum $[n_f(k)$, Eq. (63)] sum rules calculated for ^{16}O and ^{208}Pb within our extended 2NC model. The dotted and solid lines represent the values of $S_f(E)$ and $n_f(k)$ obtained by considering in Eqs. (62)–(63) the limits k_f $(E_f) \rightarrow \infty$ and using the one-hole $P_0(k,E)$ and the total $P_0(k,E)+P_1(k,E)$ spectral functions, respectively. As for $S_f(E)$, the long-dashed, dashed, and dot-dashed lines correspond to Eq. (62) calculated at $k_f=1.5$, 2.0, and 3.0 fm^{-1}, whereas in case of $n_f(k)$ they represent the results of Eq. (63) obtained at $E_f=50$, 100, and 300 MeV. For the calculation of $P_0(k,E)$ Eq. (12) has been used, with the value of the shell-model parameters taken from Ref. [35].

tion for complex nuclei obtained in Ref. [41] was not provided. On the other hand side, it has been shown [41] that the nucleon momentum distribution $n(k)$, calculated for several finite nuclei by applying the LDA to the nucleon momentum distribution in infinite nuclear matter, compares favorably with the results of many-body calculations. However, such an agreement yields only very indirect information about the removal energy dependence of the LDA spectral function. We should also stress that it is difficult to compare our spectral function with the LDA one on the basis of the calculation of inclusive cross sections (cf. Sec. V), for in the two approaches the treatment of final state interaction (FSI) is different. Indeed, in our approach [42] the FSI is such that the inclusive cross section is very sensitive upon the details of the correlated part $P_1(k,E)$ of the spectral function, whereas in [41] the inclusive nuclear response is only weakly affected by $P_1(k,E)$, when the final state interaction of the struck nucleon is considered as in Ref. [43]. To sum up, it would be very interesting to know the k and E behaviours of the LDA spectral function and to compare them with the ones obtained within our model (see, e.g., Fig. 12). In this respect we would like to stress that our spectral function provides a microscopic interpretation, in terms of two-nucleon correlations, of why the high $k-E$ behavior of the nuclear matter spectral function is as it is, i.e., featuring peaks at high values of E located at $E \propto k^2/2M$ with a FWHM given by Eq. (60).

V. *NN* CORRELATIONS AND INCLUSIVE QUASIELASTIC ELECTRON SCATTERING AT $x>1$

The effects of *NN* correlations on inclusive electron scattering has been extensively investigated in Ref. [10] for ^{3}He and [19,2,44] for complex nuclei using the plane wave impulse approximation (IA). Calculations of Refs. [19,44] have been performed using an approximated spectral function, elaborated in Ref. [45]. The present spectral function has been used for the first time in Ref. [42], where the FSI has also been taken into account. In [42] the differential cross section for inclusive quasielastic (QE) electron scattering off nuclei, $A(e,e')X$, has been evaluated at high values of the squared four momentum transfer Q^2 $[>1(\mathrm{GeV}/c)^2]$. In particular, the kinematical regions corresponding to $x>1+k_F/M \simeq 1.3$ (where k_F is the Fermi momentum and $x=Q^2/2M\nu$ the Bjorken scaling variable) have been considered, for it is in such regions that the nuclear response, evaluated within the IA, is sharply affected by the high $k-E$ components of the nuclear wave function generated by *NN* correlations (cf. Refs. [19,2]). However, it is also well known that the IA sizably underestimates the inclusive cross section at $x>1.3$ and this fact is usually ascribed to the lack of any FSI effect within the IA. In [42] the role played both by *NN* correlations and FSI has been addressed and the first results of a calculation of the inclusive cross section based upon a novel approach for evaluating FSI have been presented. Such an approach relies on a consistent treatment of *NN* correlations both in initial and final states, by extending the factorization hypothesis (45) to the final nuclear states [42].

The differential cross section for the inclusive process $A(e,e')X$ can be written in the following form:

$$\sigma^{(A)} \equiv \frac{d^2\sigma}{dE_{e'}d\Omega_{e'}} = \sigma_0^{(A)} + \sigma_1^{(A)}, \tag{67}$$

where the indices 0 and 1 have the same meaning as in Eq. (5), i.e., they distinguish the contributions resulting from dif-

ferent final nuclear states, namely $\sigma_0^{(A)}$ describes the transition to the ground and one-hole states of the $(A-1)$-nucleon system and $\sigma_1^{(A)}$ the transition to more complex highly excited configurations. In Ref. [42], the calculation of $\sigma_0^{(A)}$ and $\sigma_1^{(A)}$ has been carried out adopting different levels of sophistication for the treatment of the final A-nucleon state, starting with the IA.

The inclusive cross sections $\sigma_0^{(A)}$ and $\sigma_1^{(A)}$ within the IA reads as follows [2]:

$$[\sigma_0^{(A)}]_{\rm IA}=\sum_{N=1}^{A}\int d\vec{k}\; dE\; \sigma_{\rm eN}P_0^{(N)}(k,E)\,\delta[\nu+k^0-E_{\vec{k}+\vec{q}}], \tag{68}$$

$$[\sigma_1^{(A)}]_{\rm IA}=\sum_{N=1}^{A}\int d\vec{k}\; dE\; \sigma_{\rm eN}P_1^{(N)}(k,E)\,\delta[\nu+k^0-E_{\vec{k}+\vec{q}}], \tag{69}$$

where $\nu(\vec{q})$ is the energy (three-momentum) transfer; $\vec{k}$ is the momentum of the nucleon in the lab system before interaction and $k^0=M_A-\sqrt{(M_A+E-M)^2+k^2}$ its off-shell energy; $E_{\vec{p}}=\sqrt{M^2+|\vec{p}|^2}$; $\sigma_{\rm eN}$ is the electron- (off-shell) nucleon cross section. Using Eq. (51) for $P_1(k,E)$, Eq. (69) can be written in the following form:

$$[\sigma_1^{(A)}]_{\rm IA} =A\sigma_{\rm Mott}\sum_{N_1N_2=n,p}\int d\vec{k}_{\rm CM}\, n_{\rm CM}^{N_1N_2}(\vec{k}_{\rm CM})L^{\mu\nu}[W_{\mu\nu}^{N_1N_2}]_{\rm IA}, \tag{70}$$

where $L_{\mu\nu}$ is the (reduced) leptonic tensor and $[W_{\mu\nu}^{N_1N_2}]_{\rm IA}$ the hadronic tensor of a correlated pair, which can be written as

$$[W_{\mu\nu}^{N_1N_2}]_{\rm IA}=\frac{k^0_{\rm CM}}{2M}\sum_{f_{12}^0}\sum_{\beta_{12}}[\langle\beta_{12}|j_\mu^{N_1}+j_\mu^{N_2}|f_{12}^0\rangle]^* \times\sum_{\beta'_{12}}[\langle\beta'_{12}|j_\nu^{N_1}+j_\nu^{N_2}|f_{12}^0\rangle]\,\delta[\nu+k^0_{\rm CM} -\sqrt{(M_2^{f_{12}^0})^2+(\vec{k}_{\rm CM}+\vec{q})^2}], \tag{71}$$

where j_μ^N is the nucleon current, $k^0_{\rm CM}=M_A-\sqrt{M_{A-2}^2+|\vec{k}_{\rm CM}|^2}$, $|\beta_{12}\rangle$ is the relative wave function of the correlated pair and $|f_{12}^0\rangle$ its plane wave final state. Equation (70) is based upon the assumption that final and initial A-nucleon states factorize as follows: $|\Psi_A^f\rangle\sim\hat{A}[|f_{12}^0\rangle|\vec{P}_{\rm CM}\rangle|\Psi_{A-2}^f\rangle]$ and $|\Psi_A^0\rangle\sim\hat{A}[|\beta_{12}\rangle|\chi_{12}^{\rm CM}\rangle|\Psi_{A-2}^0\rangle]$ [cf. Eq. (45)], where $|\chi_{12}^{\rm CM}\rangle$ is the CM wave function of a correlated pair and $|\vec{P}_{\rm CM}\rangle$ its plane wave final state [note that, using Eq. (71) in Eq. (70), Eq. (69) is recovered in terms of the nucleon spectral function $P_1(k,E)$ given by Eq. (51) with $n_{\rm rel}^{N_1N_2}(\vec{k}_{\rm rel})=\Sigma_{\beta_{12}}|\langle\beta_{12}|\vec{k}_{\rm rel}\rangle|^2$]. In Ref. [42] the FSI has been evaluated by a novel approach based upon the observation that the FSI involving two nucleons emitted because of ground-state NN correlations (*two-nucleon rescattering*) should be different from the FSI involving the outgoing nucleon knocked out from shell model states (*single nucleon rescattering*).

Within the spirit of our model, at high values of k and E the absorption of the virtual photon by a correlated NN pair, which at $x>1.3$ is the dominant mechanism in the IA, is expected to resemble the one in the deuteron; if so, the deuteronlike picture of the initial state should be extended also to the final state by allowing the two nucleons to elastically rescatter. An important difference with respect to the case of the deuteron is that a correlated NN pair in a nucleus is bound and moves in the field created by the other nucleons. The basic step of our approach is the replacement of the IA hadronic tensor $[W_{\mu\nu}^{N_1N_2}]_{\rm IA}$ by the interacting one $W_{\mu\nu}^{N_1N_2}$, which is nothing but Eq. (71) with the plane wave state $|f_{12}^0\rangle$ replaced by the exact NN scattering wave function $|f_{12}\rangle$ (note that the two-nucleon rescattering process cannot be expressed in terms of a spectral function). It can be seen from Eq. (71) that medium effects on the interacting hadronic tensor are generated by the energy conserving δ function, in that the intrinsic energy available to the pair is fixed by its CM four-momentum, and, therefore, by the momentum distribution $n_{\rm CM}^{N_1N_2}$ appearing in Eq. (70); even if the CM motion is neglected [$n_{\rm CM}^{N_1N_2}=\delta(\vec{k}_{\rm CM})$] [38], medium effects still would remain through the quantity $k^0_{\rm CM}$. We have calculated the inclusive cross section for the deuteron using the Read soft core NN potential [30], taking into account the rescattering in S, P, and D partial waves; then, using the same two-nucleon amplitudes $\langle\beta_{12}|j_\mu^{N_1}+j_\mu^{N_2}|f_{12}\rangle$, we have computed the cross section $\sigma_1^{(A)}$ for complex nuclei. The results are shown by the dashed lines in Fig. 14, where the inclusive cross section for ^{2}H, ^{3}He, ^{4}He and ^{56}Fe are plotted versus the energy transfer ν at $Q^2\simeq 2({\rm GeV}/c)^2$. In Fig.15 our results expressed in terms of the nuclear scaling function $F(y,q)$ (see Ref. [2]) are plotted against the squared three-momentum transfer q^2 for fixed values of the scaling variable y [we remind the reader that $y=0$ (<0) corresponds to $x=1$ (>1)]. It can be seen that at $1.3<x<2$ the process of two-nucleon rescattering brings theoretical predictions in good agreement with the experimental data taken from Refs. [46] and [3]. The most striking aspect of our results is that the same mechanism which explains the deuteron data, does the same in a complex nucleus, provided the A dependence due to $n_{\rm CM}^{N_1N_2}$ and $k^0_{\rm CM}$ (clearly exhibited in Fig. 15) is properly considered.

However, it can also be seen from Fig. 14 that the two-nucleon rescattering is not able to describe the experimental data at $x>2$. This fact is not surprising, since at $x>2$ more than two nucleons should be involved in the scattering process. In Ref. [42] this process has been mocked up by considering the motion of the outgoing nucleon, knocked out from shell model states, in the complex optical potential generated by the ground state of the $(A-1)$-nucleon system. However, the treatment of the single-nucleon rescattering at $x>1.3$, based only on the use of on-shell optical potentials, is not justified (cf. also Refs. [38], [49], and [50]). Indeed, the struck nucleon, having four-momentum squared $p'^2\equiv(\nu+M-E)^2-(\vec{k}+\vec{q})^2$, can be either on-mass-shell ($p'^2=M^2$) or off-mass-shell ($p'^2\neq M^2$) depending on the

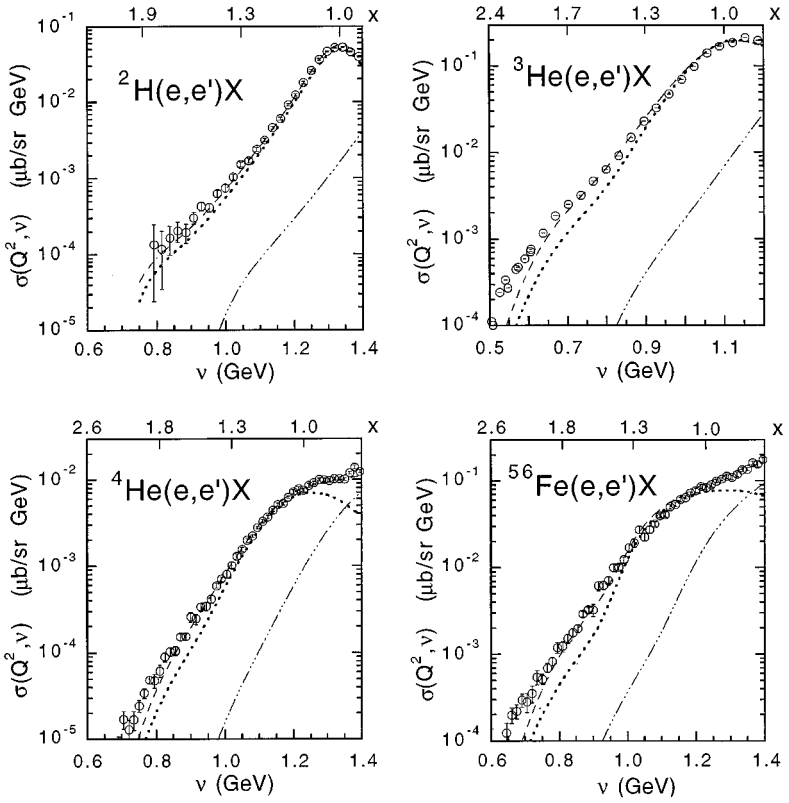

FIG. 14. Inclusive cross section $\sigma(Q^2,\nu)$ (67) for the process $A(e,e')X$ versus the energy transfer ν at $Q^2 \simeq 2(\mathrm{GeV}/c)^2$. The values of the Bjorken variable x are reported in the upper axis. The experimental data are taken from Refs. [46] and [3]. Calculations have been performed using the free nucleon form factors of Ref. [47], the $cc1$ prescription of Ref. [48] for σ_{eN} and the RSC potential [30] for the NN interaction. Dotted lines: impulse approximation [Eqs. (68) and (69)] obtained using our extended 2NC model for the nucleon spectral function. Dashed lines: IA + two-nucleon rescattering [42]. Dot-dashed lines: contribution from nucleon inelastic channels estimated as in Ref. [42].

values of k and E. Ground-state configurations with $k<|y|$ always give rise to intermediate off-shell (virtual) nucleons, whose rescattering amplitudes are expected to decrease with virtuality, for off-shell nucleons have to interact within short times. Taking into account off-shell effects as in Ref. [42], our results, including both the single-nucleon and the two-nucleon rescattering, are presented in Fig. 15. The agreement with the experimental data is good and holds in the whole low-energy side of the QE peak. To sum up, both initial state correlations and final state interaction resemble the ones occurring in the deuteron, apart from the CM motion and the binding of the pair in a complex nucleus; we have shown that the effects of NN correlations on the inclusive cross section at $x>1$ can be described by applying the factorization hypothesis to the initial as well as to the final states.

VI. *NN* CORRELATIONS AND EXCLUSIVE QUASIELASTIC ELECTRON SCATTERING

The most direct way to check our NN correlation description of the spectral function would be by exclusive experiments, in which either both k and E are measured [e.g., a $(e,e'N)$ process] or the two nucleons of the correlated pair are knocked out and detected in coincidence [e.g., a $(e,e'2N)$ process]. We briefly discuss the first process, which, as already pointed out, has provided a direct evidence of the two-nucleon correlation model [5,6]. As a matter of fact, within the IA the exclusive cross section for the process $A(e,e'p)X$ is directly proportional to the proton spectral function through

$$\frac{d^6\sigma}{dE_{e'}d\Omega_{e'}d\Omega_p dE} = KZ\sigma_{ep}[P_0(k,E)+P_1(k,E)], \quad (72)$$

where $K=p(M+T_p)(dT_p/dE_m)$ is a kinematical factor [with $p=|\vec{p}|$ (T_p) being the momentum (kinetic energy) of the detected proton] and Z is the number of protons. Within the IA one has $k=k_m$ and $E=E_m$, where k_m and E_m are the experimentally measurable missing momentum ($k_m \equiv|\vec{p}-\vec{q}|$) and missing energy ($E_m\equiv\nu-T_p-T_{A-1}$), respectively. The cross section for fixed value of k_m will therefore exhibit the shell-model structure given by the ''one-hole''spectral function P_0 [see Eq. (12)], appearing as peaks corresponding to the single-particle states located at values $E_m=|\varepsilon_\alpha|$ not affected by k_m. For large values of k_m (>1.5 fm^{-1}) one is expected to observe the structure generated by the correlated part P_1, i.e. a peak located at $E_m\sim(A-2)/(A-1)k_m^2/2M$, whose position changes with the value of k_m. Such a picture has indeed been experimen-

TABLE II. Comparison of the mean removal energy in various nuclei extracted from the energy-weighted sum rule (64) [40] ($\langle E\rangle$) with the corresponding value calculated within the extended 2NC model of the nucleon spectral function ($\langle E\rangle^{\mathrm{th}}$). The experimental values of the total binding energy per particle (ε_A) and the mean values of the nucleon kinetic energy ($\langle T\rangle$), obtained within many-body approaches, are also reported.

Nucleus	ε_A (MeV)	$\langle T\rangle$ (MeV)	$\langle E\rangle$ (MeV)	$\langle E\rangle^{\mathrm{th}}$ (MeV)
^{12}C	-7.7	32.4	44.9	44.8
^{16}O	-8.0	30.9	44.8	46.5
^{40}Ca	-8.5	33.8	50.1	49.6
^{56}Fe	-8.8	32.7	49.7	48.9
^{208}Pb	-7.9	38.2	53.7	51.8

TABLE III. Values of the parameters $A_i^{(0)}$, $B_i^{(0)}$, and $C_i^{(0)}$ appearing in the parametrization (A1) of the nucleon momentum distribution $n_0(k)$ corresponding to the ground-to-ground transition [Eq. (25)] for few-body systems.

Nucleus	^{2}H	^{3}He (proton)	^{4}He
$A_1^{(0)}$(fm^3)	157.4	31.7	4.33
$B_1^{(0)}$(fm^2)	1.24	1.32	1.54
$C_1^{(0)}$(fm^2)	18.3	5.98	0.419
$A_2^{(0)}$(fm^3)	0.234	0.00266	5.49
$B_2^{(0)}$(fm^2)	1.27	0.365	4.90
$C_2^{(0)}$(fm^2)			
$A_3^{(0)}$(fm^3)	0.00623		
$B_3^{(0)}$(fm^2)	0.220		
$C_3^{(0)}$(fm^2)			

TABLE IV. Values of the parameters $A^{(0)}$, $B^{(0)}$, $C^{(0)}$, $D^{(0)}$, $E^{(0)}$, and $F^{(0)}$ appearing in the parametrization (A1) of the "one-hole part" of the nucleon momentum distribution $n_0(k)$ [Eq. (26)] for complex nuclei and nuclear matter.

Nucleus	$A^{(0)}$ (fm^3)	$B^{(0)}$ (fm^2)	$C^{(0)}$ (fm^2)	$D^{(0)}$ (fm^4)	$E^{(0)}$ (fm^6)	$F^{(0)}$ (fm^8)
^{12}C	2.61	2.66	3.54			
^{16}O	2.74	3.33	6.66			
^{40}Ca	3.24	3.72		11.1		
^{56}Fe	3.57	4.97		19.8	15.0	
^{208}Pb	1.80	4.77		25.5		40.3
$A=\infty$ ($k<k_F$)	1.08	0.118				

tally observed in the few-nucleon systems, where only one peak is generated by P_0 at $E_m=E_{\min}$ [see Eq. (17)]. The cross sections for the processes ^{3}He$(e,e'p)X$ and ^{4}He $(e,e'p)X$, measured in Refs. [5] and [6] at various values of the proton detection angle θ_p, are presented in Fig. 16, where they are compared with our predictions within the IA [Eq. (72)] and with the results of a calculation [51,52] which also include contributions from FSI and meson exchange currents (MEC). The structure predicted by Eq. (72) is clearly seen, i.e., the two-body disintegration peak located at $E_m\simeq 5.5$ MeV in ^{3}He ($X=$ ^{2}H) and $E_{\min}\simeq 19.8$ MeV in ^{4}He ($X=$ ^{3}He) as well as the correlation peak (corresponding to $X=np$ in ^{3}He and $X=n^2H,npn$ in ^{4}He) located at $E_m\sim k^2/4M$ in ^{3}He and $E_m\sim k^2/3M$ in ^{4}He. It can be seen that the presence of FSI and MEC, which are clearly relevant at $\theta_p=90°$ in ^{3}He and $\theta_p=134°$ in ^{4}He, only affect the magnitude of the correlation peak, without sharply modify-

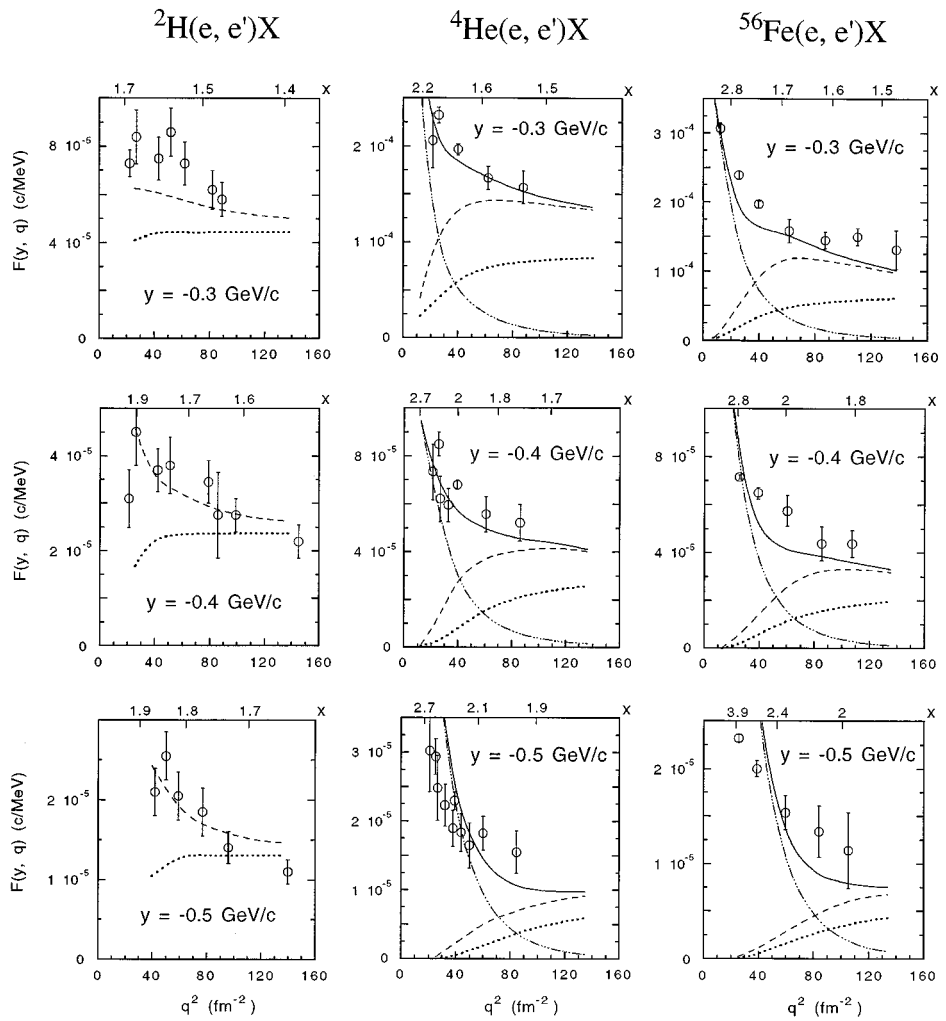

FIG. 15. Nuclear scaling function $F(y,q)$ for ^{2}H, ^{4}He, and ^{56}Fe versus the squared three-momentum transfer q^2 for fixed values of the scaling variable y [2]. The values of the Bjorken variable x are shown in the upper axis. Dotted lines: impulse approximation obtained using our extended 2NC model of the nucleon spectral function; dashed lines: correlated NN pair contribution; dot-dashed lines: *one-hole* contribution; solid line: IA + full final state interaction [42].

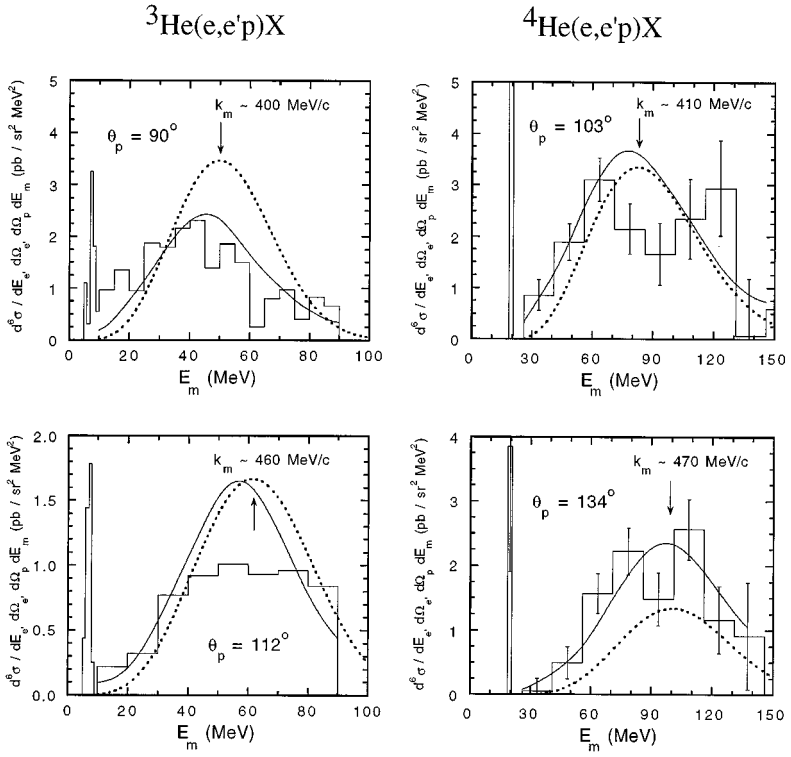

FIG. 16. Exclusive cross sections for the processes ^{3}He$(e,e'p)X$ and ^{4}He$(e,e'p)X$ versus the missing energy E_m for various values of the detection angle θ_p of the proton. The solid histograms show the data of Ref. [5] for ^{3}He and Ref. [6] for ^{4}He after radiative corrections. Dotted lines: impulse approximation [Eq. (72)] calculated using our extended 2NC model for the nucleon spectral function and adopting the free nucleon form factors of Ref. [47] and the $cc1$ prescription of Ref. [48] for σ_{ep}. Dashed lines: distorted wave impulse approximation + meson exchange currents calculated in Ref. [51] for ^{3}He and in Ref. [52] for ^{4}He. The arrows locate the values of E_m corresponding to the maxima of the cross section expected within the IA; the corresponding values of the missing momentum k_m are also reported. Note that within the IA one has $k=k_m$ and $E=E_m$.

ing its width and location. Thus the $A(e,e'N)X$ reaction off few-nucleon system is a direct confirmation of the validity of our model spectral function as well as of the original 2NC model of Ref. [38] as far as the peak location is concerned.

VII. SUMMARY AND CONCLUSIONS

We have demonstrated that at high values of k and E the nucleon spectral function can be expressed as a convolution integral involving the momentum distributions of the relative and center-of-mass motion of a correlated nucleon-nucleon pair. The basic step leading to such a convolution formula is the assumption of the factorization (45) of the nuclear wave function, which we claim to be the basic configuration which produces the high-momentum and high removal energy part of the spectral function. We have verified *a posteriori* the correctness of the factorization assumption by comparing our model spectral function with the *exact* ones in case of the three-nucleon system and infinite nuclear matter; the main outcome of such a comparison is a very good agreement in the range of energy and momentum pertaining to the region of two-nucleon correlations, which is the one investigated in the present paper. As discussed in Sec. IV, two-nucleon correlations cover a range of values of nucleon momentum k and removal energy E characterized by

$$k > 2 \ \text{fm}^{-1},$$

$$E_L < E < E^{(2)}_{\text{thr}} + \frac{A-2}{A-1}\frac{k^2}{2M}[1-2\gamma] + \sqrt{\frac{\langle k^2_{\text{CM}}\rangle 8\ \ln 2}{3}}[1-\gamma]\frac{k}{M}, \tag{73}$$

with $\gamma=[A-1/2(A-2)]\langle k^2_{\text{CM}}\rangle/\langle k^2_{\text{rel}}\rangle)$ and $E_L \sim 30$–50 MeV, which leads, e.g., for $k=2.0$, 2.5, 3.0 fm^{-1}, to 30 MeV $<E<$110, 150, 190 MeV for ^{3}He, and 50 MeV $<E<$230, 300, 380 MeV for nuclear matter, respectively. Outside this range, the effects from three-nucleon correlations (i.e., the sharing of a nucleon high-momentum component by two other nucleons) as well as from final state interaction between the recoiling nucleon and the $(A-2)$ system, is expected to modify the picture predicted by two-nucleon correlations only. As a matter of fact, the model and exact spectral functions of ^{3}He substantially differ in the region of values of E well outside the range given by Eq. (73). On the other hand side, in case of infinite nuclear matter, for which

TABLE V. Values of the parameters $A^{(1)}$, $B^{(1)}$, $C^{(1)}$, and $D^{(1)}$ appearing in the parametrization (A2) of the "correlated part" of the nucleon momentum distribution $n_1(k)$ [Eq. (24)] for various nuclei.

Nucleus	$A^{(1)}$ (fm^3)	$B^{(1)}$ (fm^2)	$C^{(1)}$ (fm^3)	$D^{(1)}$ (fm^2)
^{4}He	0.665	2.15	0.0244	0.22
^{12}C	0.426	1.60	0.0237	0.22
^{16}O	0.326	1.40	0.0263	0.22
^{40}Ca	0.419	1.77	0.0282	0.22
^{56}Fe	0.230	1.20	0.0286	0.22
^{208}Pb	0.275	1.01	0.0304	0.22
$A=\infty$ $(k<k_F)$	0.859	0.043	-0.839	0.12
$A=\infty$ $(k>k_F)$	0.432	0.97	0.0313	0.22

realistic many-body calculations include only ground-state $2p-2h$ correlations, so that the three-nucleon continuum states are absent, the model and the exact spectral functions are in very good agreement in the full range of existing calculations at $k>k_F$. Thus we are very confident that the convolution formula realistically describes the high-momentum and high removal energy parts of the nucleon spectral function in complex nuclei generated by two-nucleon correlations.

Using the convolution formula for the spectral function we have calculated the cross section for inclusive and exclusive quasielastic electron scattering off nuclei. The latter process can provide a direct check of the $k-E$ correlation dependence of the spectral function, and available data do indeed confirm the correctness of the convolution model. As for inclusive scattering, we have shown that the cross section at $x<2$ can be interpreted as due to the coupling of the virtual photon to a correlated nucleon-nucleon pair and the experimental data can quantitatively be explained provided the final state interaction is taken into account. As a final remark, we would like to point out that a direct check of the factorization assumption would provide a conclusive and stringent test of the validity of the convolution model.

ACKNOWLEDGMENTS

The authors gratefully acknowledge A. Baldo, M. Borromeo, W. Dickhoff, L.L. Frankfurt, E. Pace, A. Polls, G. Salmè, S. Scopetta, and M.I. Strikman for many fruitful discussions and enlightening remarks during the past years. Thanks are also due to O. Benhar for supplying us with the numerical output of his calculations of the nucleon spectral function in infinite nuclear matter.

APPENDIX

In this Appendix a simple parametrization of the nucleon momentum distributions $n_0(k)$ [Eq. (23)] and $n_1(k)$ [Eq. 24)], shown in Fig. 1, is presented. For $n_0(k)$ the following functional forms have been adopted:

$$n_0(k)=\sum_{i=1}^{m_0} A_i^{(0)}\frac{e^{-B_i^{(0)}k^2}}{(1+C_i^{(0)}k^2)^2} \quad \text{for } A=2,3,4$$

$$=A^{(0)}e^{-B^{(0)}k^2}[1+C^{(0)}k^2+D^{(0)}k^4+E^{(0)}k^6+F^{(0)}k^8] \quad \text{for } 4<A\leqslant\infty. \tag{A1}$$

The values of the parameters appearing in Eq. (A1) are listed in Tables III and IV. For $n_1(k)$, we have adopted a simple two-Gaussian behavior for all nuclei considered in this paper (but ^{3}He), viz.

$$n_1(k)=A^{(1)}e^{-B^{(1)}k^2}+C^{(1)}e^{-D^{(1)}k^2}. \tag{A2}$$

The values of the parameters appearing in Eq. (A2) are listed in Table V. For ^{3}He the following parametrization nicely reproduces the results of Ref. [20]:

$$n_1(k)=7.40\frac{e^{-1.23k^2}}{(1+3.21k^2)^2}+0.0139e^{-0.234k^2}, \tag{A3}$$

with k in fm^{-1} and $n_1(k)$ in fm^3. The normalization of $n_0(k)$ and $n_1(k)$ are as in Eq. (28). Finally, it should be pointed out that the quality of the parametrizations adopted is satisfactory for all nuclei considered.

[1] C. Ciofi degli Atti, S. Simula, L.L. Frankfurt, and M.I. Strikman, Phys. Rev. C **44**, R7 (1991).
[2] C. Ciofi degli Atti, E. Pace, and G. Salmé, Phys. Rev. C **43** 1153 (1991).
[3] D.B. Day *et al.*, Phys. Rev. Lett. **59**, 427 (1987); Phys. Rev. C **40**, 1011 (1989); **48**, 1849 (1993).
[4] For a review see, e.g., P.K.A. de Witt Huberts, J. Phys. G (Nucl. Part. Phys.) **16**, 507 (1990).
[5] E. Jans *et al.*, Phys. Rev. Lett. **49**, 974 (1982); E. Jans *et al.*, Nucl. Phys. **A475**, 687 (1987); C. Marchand *et al.*, Phys. Rev. Lett. **60**, 1703 (1988).
[6] J.M. Le Goff *et al.*, Phys. Rev. C **50**, 2278 (1994).
[7] R.W. Lourie *et al.*, Phys. Rev. Lett. **56**, 2364 (1986); P.E. Ulmer *et al.*, *ibid*. **59**, 2259 (1987); **61**, 2001 (1988); H. Baghaei *et al.*, Phys. Rev. C **39**, 177 (1989); L.B. Weinstein *et al.*, Phys. Rev. Lett. **64**, 1646 (1990).
[8] L.J.H.M. Kester *et al.*, Phys. Lett. B **344** 79 (1995).
[9] H. Meier-Hajduk, P.U. Sauer, and W. Theis, Nucl. Phys. **A395**, 332 (1983).
[10] C. Ciofi degli Atti, E. Pace, and G. Salmé, Phys. Rev. C **21**, 805 (1980).
[11] O. Benhar, A. Fabrocini, and S. Fantoni, Nucl. Phys. **A505**, 267 (1989); **A550**, 201 (1992).
[12] A. Ramos, A. Polls, and W.H. Dickhoff, Nucl. Phys. **A503**, 1 (1989); W.H. Dickhoff and H. Muther, Rep. Prog. Phys. **55**, 1947 (1992); B.E. Vonderfecht, W.H. Dickhoff, A. Polls, and A. Ramos, Phys. Rev. C **41**, R1265 (1991); Nucl. Phys. **A555**, 1 (1993).
[13] H.S. Kohler, Nucl. Phys. **A537**, 64 (1992); Phys. Rev. C **46**, 1687 (1992).

[14] C. Mahaux and R. Sartor, Nucl. Phys. **A546**, 65c (1992); M. Baldo, I. Bombaci, G. Giansiracusa, U. Lombardo, C. Mahaux, and R. Sartor, **A545**, 741 (1992).
[15] F. de Jong and R. Malfliet, Phys. Rev. C **44**, 998 (1991).
[16] P. Fernández de Córdoba and E. Oset, Phys. Rev. C **46**, 1697 (1992).
[17] H. Morita and T. Suzuki, Prog. Theor. Phys. **86**, 671 (1991).
[18] H. Muther and W.H. Dickhoff, Phys. Rev. C **49**, R17 (1994); W.H. Dickhoff and A. Polls (private communication).
[19] C. Ciofi degli Atti, S. Liuti, and S. Simula, Phys. Rev. C **41**, R2474 (1990).
[20] C. Ciofi degli Atti, E. Pace, and G. Salmé, Phys. Lett. **141B**, 14 (1984).
[21] Y. Akaishi, Nucl. Phys. **A416**, 409c (1984); H. Morita, Y. Akaishi, and H. Tanaka, Prog. Theor. Phys. **79**, 863 (1988).
[22] S. Fantoni and V.R. Pandharipande, Nucl. Phys. **A427**, 473 (1984).
[23] R. Schiavilla, V.R. Pandharipande, and R.B. Wiringa, Nucl. Phys. **A449**, 219 (1986); R.B. Wiringa, Phys. Rev. C **43**, 1585 (1991).
[24] O. Benhar, C. Ciofi degli Atti, S. Liuti, and G. Salmé, Phys. Lett. B **177**, 135 (1986).
[25] S.C. Pieper, R.B. Wiringa, and V.R. Pandharipande, Phys. Rev. C **46**, 1741 (1992).
[26] X. Ji and J. Engel, Phys. Rev. C **40**, R497 (1989).
[27] M. Jaminon, C. Mahaux, and H. Ngo, Nucl. Phys. **A452**, 445 (1986).
[28] J.G. Zabolitzky and W. Ey, Phys. Lett. **76B**, 527 (1978).
[29] J.W. Van Orden, W. Truex, and M.K. Banerjee, Phys. Rev. C **21**, 2628 (1980).
[30] R.V. Reid, Ann. Phys. (N.Y.) **50**, 411 (1968).
[31] M. Lacombe *et al.*, Phys. Rev. C **21**, 861 (1980).
[32] R.B. Wiringa, R.A. Smith, and T.L. Ainsworth, Phys. Rev. C **29**, 1207 (1984).
[33] M. Berheim *et al.*, Nucl. Phys. **A365**, 349 (1981); S. Turck-Chieze *et al.*, Phys. Lett. B **142**, 145 (1984).
[34] J.F.J. Van Den Brandt *et al.*, Phys. Rev. Lett. **60**, 2006 (1988); A. Magnon *et al.*, Phys. Lett. B **222**, 352 (1989).
[35] S. Frullani and J. Mougey, Adv. Nucl. Phys. **14**, 1 (1984).
[36] H. Morita, Y. Akaishi, and H. Tanaka, Prog. Theor. Phys. **79**, 863 (1988).
[37] J. Carlson, V.R. Pandharipande, and R. Schiavilla, Phys. Rev. C **47**, 484 (1993); R. Schiavilla, in Proceedings of the 6th Workshop on Perspectives in Nuclear Physics at Intermediate Energies, ICTP (Trieste, Italy), May 8-12, 1995, edited by. S. Boffi, C. Ciofi degli Atti, and M. Giannini (World Scientific Publishing, Singapore, in press).
[38] L.L. Frankfurt and M.I. Strikman, Phys. Rep. **76**, 215 (1981); **160**, 235 (1988).
[39] C. Ciofi degli Atti, E. Pace, and G. Salmé, in *Few Body Systems and Electromagnetic Interactions*, edited by C. Ciofi degli Atti and E. de Sanctis, Lecture Notes in Physics Vol. 86 (Springer, Berlin, 1978), p. 316.
[40] D.S. Koltun, Phys. Rev. C **9**, 484 (1974); S. Boffi, Lett. Nuovo Cimento **1**, 971 (1971).
[41] (a) I. Sick, S. Fantoni, A. Fabrocini, and O. Benhar, Phys. Lett. B **323**, 267 (1994); (b) O. Benhar, A. Fabrocini, S. Fantoni, and I. Sick, Nucl. Phys. **A579**, 493 (1994).
[42] C. Ciofi degli Atti and S. Simula, Phys. Lett. B **325**, 276 (1994); and (unpublished).
[43] O. Benhar, A. Fabrocini, S. Fantoni, G.A. Miller, V.R. Pandharipande, and I. Sick, Phys. Rev. C **44**, 2328 (1991).
[44] C. Ciofi degli Atti, D.B. Day, and S. Liuti, Phys. Rev. C **46**, 1045 (1992).
[45] C. Ciofi degli Atti, L.L. Frankfurt, S. Simula, and M.I. Strikman, in *Proceedings of the 4th Workshop on Perspectives in Nuclear Physics at Intermediate Energies*, ICTP (Trieste, Italy), May 8–12 1989, edited by. S. Boffi, C. Ciofi degli Atti, and M. Giannini (World Scientific Publishing, Singapore, 1989), p. 312.
[46] W. Schutz *et al.*, Phys. Rev. Lett. **38**, 259 (1977); S. Rock *et al.*, *ibid*. **49**, 1139 (1982); S. Rock (private communication).
[47] S. Galster *et al.*, Nucl. Phys. **B32**, 221 (1971).
[48] T. de Forest, Nucl. Phys. **A392**, 232 (1983).
[49] L.L. Frankfurt, M.I. Strikman, D.B. Day, and M. Sargsyan, Phys. Rev. C **48**, 2451 (1993).
[50] T. Uchiyama, A.E.L. Dieperink, and O. Scholten, Phys. Lett. B **233**, 31 (1989).
[51] J.M. Laget, Phys. Lett. **151B**, 325 (1985).
[52] J.M. Laget, in *New Vistas in Electronuclear Physics*, edited by E. Tomusiak (Plenum, New York, 1986), p. 361.